17. Takegawa, Y., Deguchi, K., Ito, S., Yoshioka, S., Sano, A., Yoshinari, K., Kobayashi, K., Nakagawa, H., Monde, K., and Nishimura, S. (2004) Anal Chem. **76**, 7294–7303
18. Takegawa, Y., Deguchi, K., Ito, S., Yoshioka, S., Nakagawa, H., and Nishimura, S. (2005) Rapid Commun. Mass Spectrom. **19**, 937–946
19. Harvey, D. J. (1999) Mass Spectrom. Rev. **18**, 349–450
20. Harvey, D. J., Bateman, R. H., and Green, M. R. (1997) J. Mass Spectrom. **32**, 167–187
21. Kawasaki, N., Ohta, M., Hyuga, S., Hashimoto, O., and Hayakawa, T. (1999) Anal. Biochem. **269**, 297–303
22. Kawasaki, N., Haishima, Y., Ohta, M., Itoh, S., Hyuga, M., Hyuga, S., and Hayakawa, T. (2001) Glycobiology **11**, 1043–1049
23. Sato, Y., Suzuki, M., Nirasawa, T., Suzuki, A., and Endo, T. (2000) Anal. Chem. **72**, 1207–1216
24. Takegawa, Y., Deguchi, K., Ito, S., Yoshioka, S., Nakagawa, H., and Nishimura, S. (2005) Anal. Chem. **77**, 2097–2106
25. Royle, L., Mattu, T. S., Hart, E., Langridge, J. I., Merry, A. H., Murphy, N., Harvey, D. J., Dwek, R. A., and Rudd, P. M. (2002) Anal. Biochem. **304**, 70–90
26. Hase, S., Ikenaka, T., and Matsushima, Y. (1981) J. Biochem. (Tokyo). **90**, 407–414
27. Suzuki-Sawada, J., Umeda, Y., Kondo, A., and Kato, I. (1992) Anal. Biochem. **207**, 203–207
28. Bigge, J. C., Patel, T. P., Bruce, J. A., Goulding, P. N., Charles, S. M., and Parekh, R. B. (1995) Anal. Biochem. **230**, 229–238
29. Ohta, M., Hamako, J., Yamamoto, S., Hatta, H., Kim, M., Yamamoto, T., Oka, S., Mizuochi, T., and Matsuura, F. (1991) Glycoconj. J. **8**, 400–413
30. Yoshimi, Y., Yamazaki, S., and Ikekita, M. (1999) Biochem. Biophys. Acta. **1426**, 69–79
31. Suzuki, S., Kakehi, K., and Honda, S. (1996) Anal. Chem. **68**, 2073–2083
32. Okamoto, M., Takahashi, K., and Doi, T. (1995) Rapid Commun. Mass Spectrom. **9**, 641–643
33. Lattova, E., and Perreault, H. (2003) J. Chromatogr. A. **1016**, 71–87
34. Morelle, W., Faid, V., and Michalski, J. C. (2004) Rapid Commun. Mass Spectrom. **18**, 2451–2464
35. Yoshino, K., Takao, T., Murata, H., and Shimonishi, Y. (1995) Anal. Chem. **67**, 4028–4031
36. Kawasaki, N., Ohta, M., Itoh, S., Hyuga, M., Hyuga, S., and Hayakawa, T. (2002) Biologicals. **30**, 113–123
37. Karlsson, N. G., Wilson, N. L., Wirth, H. J., Dawes, P., Joshi, H., and Packer, N. H. (2004) Rapid Commun. Mass Spectrom. **18**, 2282–2292
38. Zamfir, A., Seidler, D. G., Schonherr, E., Kresse, H., and Peter-Katalinic, J. (2004) Electrophoresis **25**, 2010–2016
39. Kremmer, T., Szollosi, E., Boldizsar, M., Vincze, B., Ludanyi, K., Imre, T., Schlosser, G., and Vekey, K. (2004) Biomed. Chromatogr. **18**, 323–329
40. Hashii, N., Kawasaki, N., Itoh, S., Hyuga, M., Kawanishi, T., and Hayakawa, T. (2005) Proteomics (in press)
41. Yuan, J., Hashii, N., Kawasaki, N., Itoh, S., Kawanishi, T., and Hayakawa, T. (2005) J. Chromatogr. A. **1067**, 145–152
42. Demelbauer, U. M., Zehl, M., Plematl, A., Allmaier, G., and Rizzi, A. (2004) Rapid Commun. Mass Spectrom. **18**, 1575–1582
43. Roepstorff, P., and Fohlman, J. (1984) Biomed. Mass Spectrom. **11**, 601
44. Hakansson, K., Chalmers, M. J., Quinn, J. P., McFarland, M. A., Hendrickson, C. L., and Marshall, A. G. (2003) Anal. Chem. **75**, 3256–3262
45. Hakansson, K., Cooper, H. J., Emmett, M. R., Costello, C. E., Marshall, A. G., and Nilsson, C. L. (2001) Anal. Chem. **73**, 4530–4536
46. Kurogochi, M., and Nishimura, S. (2004) Anal. Chem. **76**, 6097–6101
47. Krokhin, O., Ens, W., Standing, K. G., Wilkins, J., and Perreault, H. (2004) Rapid Commun. Mass Spectrom. **18**, 2020–2030
48. Wuhrer, M., Hokke, C. H., and Deelder, A. M. (2004) Rapid Commun. Mass Spectrom. **18**, 1741–1748
49. Harazono, A., Kawasaki, N., Kawanishi, T., and Hayakawa, T. (2005) Glycobiology **15**, 447–462
50. Nemeth, J. F., Hochgesang, G. P., Jr., Marnett, L. J., and Caprioli, R. M. (2001) Biochemistry **40**, 3109–3116
51. Hui, J. P., White, T. C., and Thibault, P. (2002) Glycobiology **12**, 837–849
52. Sandra, K., Devreese, B., Van Beeumen, J., Stals, I., and Claeyssens, M. (2004) J. Am. Soc. Mass Spectrom. **15**, 413–423
53. Sandra, K., Stals, I., Sandra, P., Claeyssens, M., Van Beeumen, J., and Devreese, B. (2004) J. Chromatogr. A. **1058**, 263–272
54. Satomi, Y., Shimonishi, Y., and Takao, T. (2004) FEBS Lett. **576**, 51–56
55. Wada, Y., Tajiri, M., and Yoshida, S. (2004) Anal. Chem. **76**, 6560–6565
56. Itoh, S., Kawasaki, N., Hashii, N., Harazono, A., Matsuishi, Y., Kawanishi, T., and Hayakawa, T. (2005) J. Chromatogr. A. Submitted
57. Garcia, R., Rodriguez, R., Montesino, R., Besada, V., Gonzalez, J., and Cremata, J. A. (1995) Anal. Biochem. **231**, 342–348
58. Fu, D., and van Halbeek, H. (1992) Anal. Biochem. **206**, 53–63
59. Carr, S. A., Huddleston, M. J., and Bean, M. F. (1993) Protein Sci. **2**, 183–196
60. Ethier, M., Saba, J. A., Spearman, M., Krokhin, O., Butler, M., Ens, W., Standing, K. G., and Perreault, H. (2003) Rapid Commun. Mass Spectrom. **17**, 2713–2720
61. Huddleston, M. J., Bean, M. F., and Carr, S. A. (1993) Anal. Chem. **65**, 877–884
62. Kapron, J. T., Hilliard, G. M., Lakins, J. N., Tenniswood, M. P., West, K. A., Carr, S. A., and Crabb, J. W. (1997) Protein Sci. **6**, 2120–2133
63. Medzihradszky, K. F., Besman, M. J., and Burlingame, A. L. (1997) Anal. Chem. **69**, 3986–3994
64. Ritchie, M. A., Gill, A. C., Deery, M. J., and Lilley, K. (2002) J. Am. Soc. Mass Spectrom. **13**, 1065–1077
65. Schindler, P. A., Settineri, C. A., Collet, X., Fielding, C. J., and Burlingame, A. L. (1995) Protein Sci. **4**, 791–803
66. Wang, F., Nakouzi, A., Angeletti, R. H., and Casadevall, A. (2003) Anal. Biochem. **314**, 266–280
67. Wilson, N. L., Schulz, B. L., Karlsson, N. G., and Packer, N. H. (2002) J. Proteome Res. **1**, 521–529
68. Itoh, S., Harazono, A., Kawasaki, N., Hashii, N., Matsuishi, Y., Kawanishi, T., and Hayakawa, T. (2004) J. Electrophoresis **48**, 163–168
69. Fan, X., She, Y. M., Bagshaw, R. D., Callahan, J. W., Schachter, H., and Mahuran, D. J. (2004) Anal. Biochem. **332**, 178–186
70. Higai, K., Shibukawa, K., Muto, S., and Matsumoto, K. (2003) Anal. Sci. **19**, 85–92
71. Kaji, H., Saito, H., Yamauchi, Y., Shinkawa, T., Taoka, M., Hirabayashi, J., Kasai, K., Takahashi, N., and Isobe, T. (2003) Nat. Biotechnol. **21**, 667–672
72. Qiu, R., and Regnier, F. E. (2005) Anal. Chem. **77**, 2802–2809

Received on June 3, 2005, accepted on July 19, 2005

©2005 FCCA (Forum: Carbohydrates Coming of Age)

Profile of the Author

Nana Kawasaki studied organic chemistry and received MS degree from Faculty of Pharmaceutical Sciences, Hokkaido University in 1986. She joined the Division of Biological Chemistry & Biologicals, the National Institute of Health Sciences in 1986. She obtained her PhD from Hokkaido University in 1996. Her current research focuses on a development of evaluation methods of glycoprotein products by mass spectrometry.

©2005 FCCA (Forum: Carbohydrates Coming of Age)

FCCA MEMBERSHIP APPLICATION FORM (入会申込書)

(コピーしてお使いください。Please photocopy this page)

A. Domestic (国内会員)

正会員(5,000円)、学生会員(3,000円)、賛助会員(50,000円)、団体会員(図書館)(20,000円)の会員種別を銘記のうえ郵便局より口座番号00100-8-123251(加入者名FCCA)宛該当会費をお振り込みください。同時に受領書のコピーおよび下記会員情報カードにご記入のうえFCCA事務局まで、郵送またはFAXにてお送りください。

〒564-0062　大阪府吹田市垂水町1-1-8　学進出版内　FCCA事務局　FAX: 06-6330-2724

B. Overseas(海外会員)

The membership fee for student and regular member is payable only by credit card. Please fill in the following application form legibly(type or print) and return to:

FCCA Head Office, c/o Gakushin Publishing Co. Ltd., 1-1-8 Tarumi-cho, Suita 564-0062, Osaka, Japan
FAX: 81-6-6330-2724

Register as a (check one box)
☐ Student membership (Overseas: ¥5,000)
☐ Regular membership (Overseas: ¥7,000)
☐ Institutional membership (Overseas: ¥22,000)
☐ Supporting membership (Overseas: ¥52,000)

Charge my (check one box)
☐ AMERICAN EXPRESS
☐ DINERS
☐ MASTERCARD
☐ VISA

Card No.:

Expiration Date:

Name in Full (Please type or print):

Years you wish to pay: 2001, 2002, 2003 (Please circle your choices)

Signature:

FCCA Membership Information Card

フリガナ 氏名 (Name)		( )	生年月日（西暦） Birth date Year Month Day
自宅住所 Home address		〒 Tel.: Fax.:	会員種別 Type of Membership □ 1 正会員Regular □ 2 学生Student □ 3 賛助Supporting □ 4 団体Institutional 維持Sustaining
所属機関	名称 Office or Lab.		
	住所 Address Country	〒 E-mail：	職名: Professional title Tel.: Fax.:
最終学歴 Education		大学 Univ. □学士Bachelor □修士Master □博士Doctor Year graduated: 年卒 □その他Others (explain):	□ 糖質学会会員
連絡先 Contact preference		国内domestic 所属機関 □ 1 自宅住所 □ 2 海外abroad □ 3 Office □ 4 Home	研究分野 Areas of interest

ELSEVIER

Available online at www.sciencedirect.com

SCIENCE DIRECT

Journal of Chromatography A, 1103 (2006) 296–306

JOURNAL OF CHROMATOGRAPHY A

www.elsevier.com/locate/chroma

N-linked oligosaccharide analysis of rat brain Thy-1 by liquid chromatography with graphitized carbon column/ion trap-Fourier transform ion cyclotron resonance mass spectrometry in positive and negative ion modes

Satsuki Itoh[a], Nana Kawasaki[a,b,*], Noritaka Hashii[b], Akira Harazono[a], Yukari Matsuishi[a], Takao Hayakawa[c], Toru Kawanishi[a]

[a] *Division of Biological Chemistry and Biologicals, National Institute of Health Science, 1-18-1 Kamiyoga, Setagaya-ku, Tokyo 158-8501, Japan*
[b] *CREST, Japan Science and Technology Agency (JST), Japan*
[c] *Pharmaceutical and Medical Devices Agency, 3-3-2 Kasumigaseki, Chiyoda-ku, Tokyo 100-0013, Japan*

Received 25 July 2005; received in revised form 10 November 2005; accepted 14 November 2005
Available online 20 December 2005

Abstract

We have previously described the site-specific glycosylation analysis of rat brain Thy-1 by LC/multistage tandem mass spectrometry (MS^n) using proteinase-digested Thy-1. In the present study, detailed structures of oligosaccharides released from Thy-1 were elucidated by mass spectrometric oligosaccharide profiling using LC/MS with a graphitized carbon column (GCC–LC/MS). First, using model oligosaccharides, we improved the oligosaccharide profiling by ion trap mass spectrometry (IT–MS) coupled with Fourier transform ion cyclotron resonance mass spectrometry (FT–ICR–MS). Sequential scanning of a full MS^1 scan with FT–ICR–MS followed by data-dependent MS^n with IT–MS in positive ion mode, and a subsequent full MS^1 scan with FT–ICR–MS followed by data-dependent MS^n with IT–MS in negative ion mode enabled the monosaccharide composition analysis as well as profiling and sequencing of both neutral and acidic oligosaccharides in a single analysis. The improved oligosaccharide profiling was applied to elucidation of N-linked oligosaccharides from Thy-1 isolated by sodium dodecyl sulfate-polyacrylamide gel electrophoresis. It was demonstrated that Thy-1 possesses a significant variety of N-linked oligosaccharides, including Lewis a/x, Lewis b/y, and disialylated structure as a partial structure. Our method could be applicable to analysis of a small abundance of glycoproteins, and could become a powerful tool for glycoproteomics.
© 2005 Elsevier B.V. All rights reserved.

Keywords: Mass spectrometric oligosaccharide profiling; Graphitized carbon column; Ion trap mass spectrometry; Fourier transform ion cyclotron resonance mass spectrometry; Data-dependent MS^n; Thy-1

1. Introduction

Glycosylation is one of the most abundant post-translational modifications of proteins [1]. It is already known that glycosylation influences the biological functions as well as the physicochemical properties of proteins, i.e., folding, solubility, aggregation, and stability. A number of reports have noted a positive relationship between a change in glycosylation and development, aging, and certain diseases [2–4]. Elucidation of structural detail in oligosaccharides is necessary to clarify the biological properties of glycoproteins.

MS is now a powerful tool for structural analysis of glycoproteins. There are two major mass spectrometric approaches to the structural analysis of glycoproteins, i.e., MS of glycopeptides [5–7] and of oligosaccharides [8–13]. For oligosaccharide sequencing, tandem mass spectrometry as well as exoglycosidase digestions in conjuction with MS is recognized as an effective means of oligosaccharide sequencing [14–16]. Mass spectrometric peptide/glycopeptide mapping by LC coupled with tandem mass spectrometry (LC/MS/MS) is effective for the determination of glycosylation sites and the analysis of site-specific heterogeneity [17–22]. However, structural detail in

---

* Corresponding author. Division of Biological Chemistry and Biologicals, National Institute of Health Science, 1-18-1, Kamiyoga, Setagaya-ku, Tokyo 158-8501, Japan. Tel.: +81 3 3700 1141; fax: +81 3 3707 6950.
E-mail address: nana@nihs.go.jp (N. Kawasaki).

0021-9673/$ – see front matter © 2005 Elsevier B.V. All rights reserved.
doi:10.1016/j.chroma.2005.11.043

oligosaccharides is not always available by product ion spectra of glycopeptides, as many of the precursor ions consist of uniform peptides carrying different oligosaccharides with identical *m/z* values. LC/MS/MS of glycopeptides has limitations for the structural analysis of carbohydrates due to the difficulty of isolating of glycopeptide isomers. Mass spectrometric oligosaccharide profiling through the separation of isomers by LC can supply the structural detail of each oligosaccharide although it cannot provide information regarding glycosylation sites and site-specific glycosylation [23–29]. MS of both glycopeptides and oligosaccharides is needed for glycosylation analysis of a glycoprotein [30].

Thy-1 is a cell adhesion molecule that belongs to the immunoglobulin superfamily and is attached to the cell membrane via a glycosylphosphatidylinositol (GPI)-anchor. We recently, studied the glycosylation of Thy-1 in rat brain by mass spectrometric peptide/glycopeptide mapping, and demonstrated that Thy-1 possesses various *N*-glycans at Asn23, 74, and 98 [31]. The monosaccharide composition of *N*-glycan at each glycosylation site was estimated by masses of molecular ions; however, structural detail regarding some of the oligosaccharides could not be elucidated by MS^n since many glycopeptides with identical *m/z* values contained several oligosaccharide isomers and yielded product ions from a mixture of these glycopeptide isomers. Mass spectrometric oligosaccharide profiling is necessary for detailed structural analysis of oligosaccharides.

We have previously demonstrated a simple means of oligosaccharide profiling using liquid chromatography/electrospray ionization mass spectrometry with a graphitized carbon column (GCC–LC/MS) [32–34], in which oligosaccharides can be separated on the basis of their branching, sequence, and linkage, and can be characterized based on their monosaccharide compositions estimated from their calculated molecular masses. Here, we study the glycosylation of Thy-1 by oligosaccharide profiling with GCC–LC/MS. First, we improved our oligosaccharide profiling by ion trap mass spectrometry (IT–MS) coupled with Fourier transform ion cyclotron resonance mass spectrometry (FT–ICR–MS). This instrument is capable of both monosaccharide composition analysis by acquisition of accurate masses and data-dependent multistage tandem MS (MS^n) for sequencing with fast switching between positive and negative ion modes. Using a mixture of typical oligosaccharides, including high-mannose-type, and asialo-, trisialylated, and tetrasialylated complex-types, we confirmed that the improved method can be used for monosaccharide composition analysis and detailed structural analysis of both neutral and acidic oligosaccharides. The method was then applied to N-linked oligosaccharide analysis of rat brain Thy-1.

2. Experimental

2.1. Materials

Man7/D1, Man7/D3, and asialo-triantennary (Tri) were obtained from Oxford Glycosystems (Abingdon, UK). Trisialylated triantennary (TriNA$_3$) and tetrasialylated tetraantennary (TetraNA$_4$) were purchased from Dionex (Sunnyvale, CA, USA). Rat brain was purchased from Nippon SLC (Hamamatsu, Japan). Phosphatidylinositol-specific phospholipase C (PIPLC) from *Bacillus cereus* was purchased from Molecular Probes (Eugene, OR, USA). Peptide-*N*-glycosidase F (PNGase F) was purchased from Roche Diagnostics (Mannheim, Germany). SimplyBlue SafeStain was obtained from Invitrogen (Carlsbad, CA, USA).

2.2. Release of N-linked oligosaccharides from rat brain Thy-1 by in-gel PNGase F digestion

PIPLC-treated GPI-anchored proteins were prepared from rat brain as reported previously [31]. Briefly, the homogenate of rat brain was defatted and solubilized with 2% Triton X-114 at 4 °C overnight [35,36]. After centrifugation, the supernatant was subjected to Triton X-114 phase-partitioning at 37 °C. Solubilized membrane proteins in the detergent phase were precipitated with cold acetone, and the precipitates were digested with PIPLC. After resubjecting the digest mixture to Triton X-114 phase-partitioning, PIPLC-treated soluble GPI-anchored proteins in aqueous phase were precipitated by adding cold acetone. These proteins were carboxyamidomethylated [30], and were separated by sodium dodecyl sulfate–polyacrylamide gel electrophoresis (SDS–PAGE) (12.5%) followed by staining with SimplyBlue SafeStain.

In-gel PNGase F digestion of Thy-1 and extraction of N-linked oligosaccharides were performed as previously described

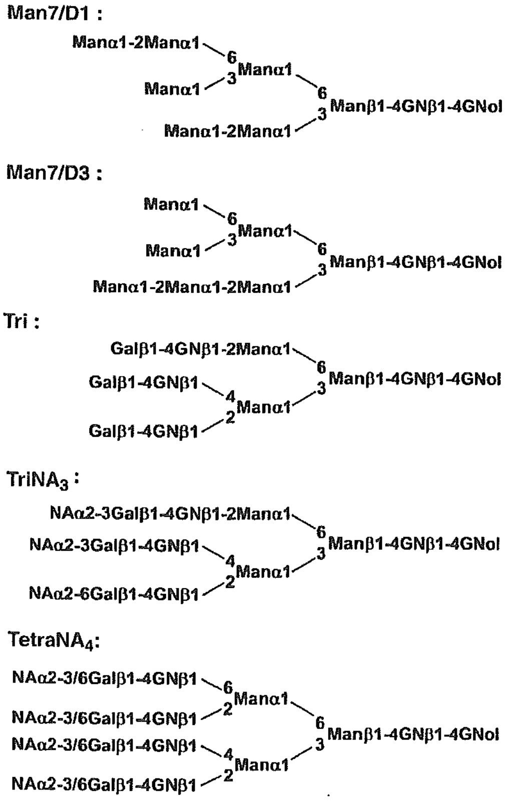

Fig. 1. Structures of major oligosaccharides and their abbreviations. Man: mannose, Gal: galactose, GN; *N*-acetylglucosamine, GNol; *N*-acetylglucosaminitol, NA; *N*-acetylneuramic acid.

[15]. The protein band of Thy-1 (20–25 kDa) was excised, cut into pieces, and destained. The gel pieces were dehydrated with 50% acetonitrile. The dried gels were then equilibrated with 50 mM sodium phosphate buffer (pH 7.2) and incubated at 37 °C with 3 units of PNGase F. The released *N*-glycans were extracted three times from gel pieces by intermittent sonication for 30 min in water. All extracts were combined and lyophilized. The released N-linked oligosaccharides were reduced with $NaBH_4$, as previously reported [33], and subjected to GCC–LC/IT–MS-FT–ICR–MS.

2.3. N-linked oligosaccharide analysis by GCC–LC/IT-MS-FT–ICR–MS

GCC–LC/MS was carried out using a MAGIC 2002 system (Michrom BioResource, Auburn, CA, USA) connected to IT–MS instrument coupled with FT–ICR–MS instrument (Finnigan LTQ FT, Thermo Electron Corp., San Jose, CA, USA). The eluents consisted of 5 mM ammonium acetate, pH 9.6, containing 2% CH_3CN (pump A), and 5 mM ammonium acetate, pH 9.6, containing 80% CH_3CN (pump B). The borohydride-reduced N-linked oligosaccharides were separated on Hypercarb (150 mm × 0.2 mm, 5 μm, Thermo Electron Corp.) as GCC with a linear gradient of 5–30% for pump B over a period of 60 min at a flow rate of 2 μl/min.

The MS^n experiment includes sequential scans, as follows: a full MS^1 scan (*m/z* 700–2000) by FT–ICR–MS in positive ion mode, data-dependent MS^n scans by IT–MS for most abundant ions regardless of their charge state, a full MS^1 scan (*m/z* 700–2000) by FT–ICR–MS in negative ion mode, and data-dependent MS^n scans by IT–MS for the most intense ions regardless of their charge state. For the data-dependent MS^n, the following settings were used: the isolation window for precursor masses, ±2.5 Da; collision energy, 35%; dynamic exclusion

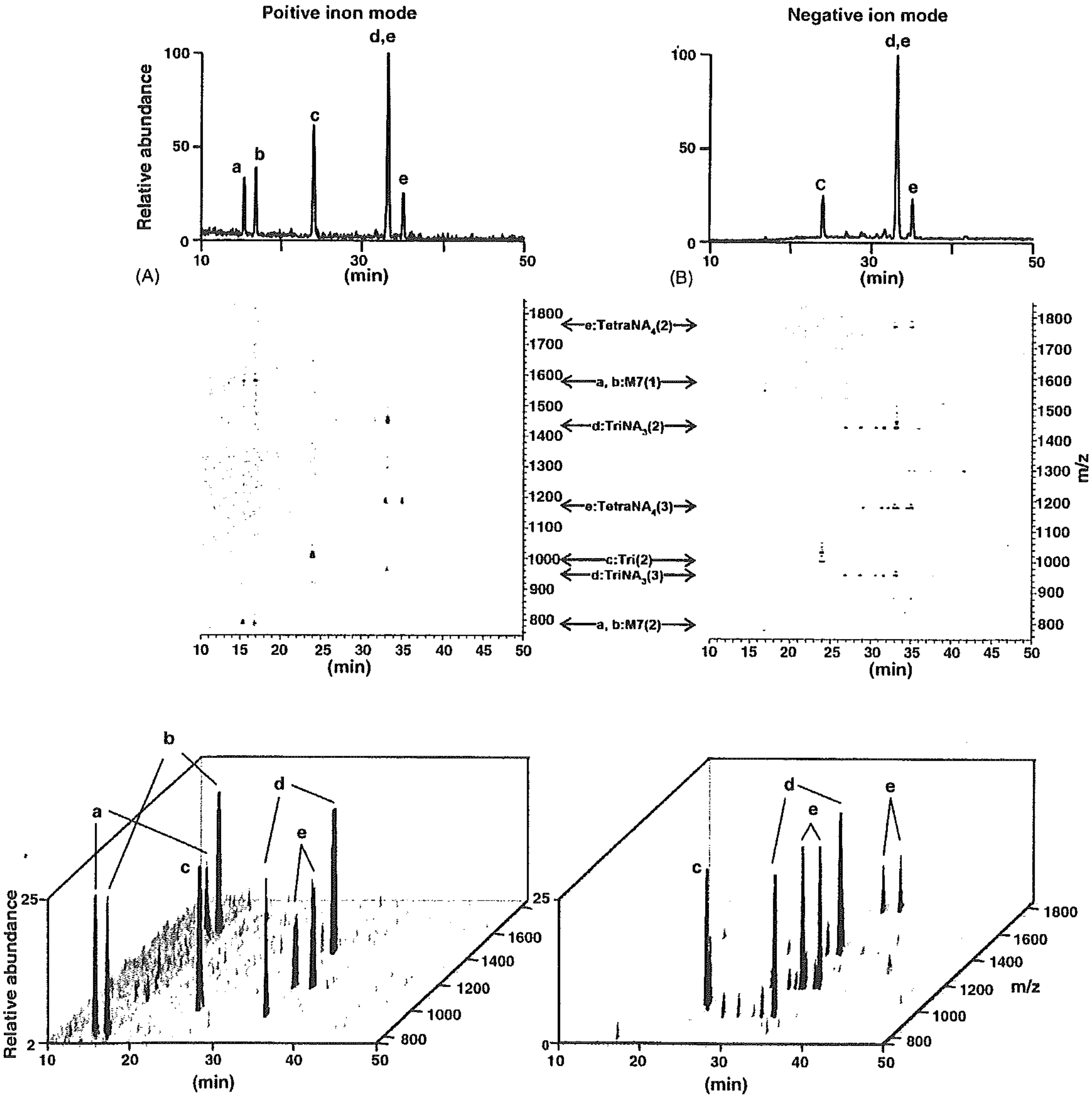

Fig. 2. Typical oligosaccharide profiles obtained by full MS^1 scans with FT–ICR–MS. (A) total ion chromatogram (TIC) (upper), two-dimensional (2D) display (retention time vs. *m/z*) (middle), and three-dimensional (3D) display (lower) in positive ion mode. (B) TIC (upper), 2D (middle) and 3D display (lower) in negative ion mode. Numbers in parentheses after the abbreviation of the model oligosaccharides refer to the charge state.

time, 15 s. The operating conditions employed for LC/MS^n were as follows: tube lens offset, 120 V; capillary voltage, 2.0 kV; and capillary temperature, 200 °C.

3. Results

3.1. GCC-LC/IT-MS-FT-ICR-MS of model oligosaccharides

By using the IT–MS-FT–ICR-MS instrument, the oligosaccharide profiling was shown to be more rapid, accurate, and informative. Man7/D1, Man7/D3, Tri, TriNA$_3$, and TetraNA$_4$, which were chosen as model neutral and acidic oligosaccharides (Fig. 1), were analyzed by alternative scans in positive and negative ion modes, which are consisting of a full MS^1 scan by FT–ICR–MS followed by data-dependent MS^n scans by IT–MS. Fig. 2A and B show the oligosaccharide profiles obtained by a full MS^1 scan with FT–ICR–MS (*m/z* 700–2000) in positive and negative ion modes, respectively. The monosaccharide compositions of individual oligosaccharides could be easily determined by accurate *m/z* values, and the major peaks of a, b, c, d, and e were assigned to Man7/D1 or D3, Man7/D3 or D1, Tri, TriNA$_3$ and TetraNA$_4$, respectively. Oligosaccharides detected at the same *m/z* values are positional isomers. Man7/D1 and D3 were detected in positive ion mode, but were only slightly detectable in negative ion mode. The major isomers of TriNA$_3$ and TetraNA$_4$ were detected in both ion modes, whereas their minor isomers were detected only in negative ion mode. These results demonstrate the advantage of alternative scans in both ion modes.

We confirmed the possibility of data-dependent MS^n scans for sequencing neutral and sialylated oligosaccharides. Man 7/D1 and D3 could be distinguished from each other by data-dependent MS^n (Fig. 3). Oligosaccharide eluted at 15 min could be assigned to Man7/D1 by the relatively intense ions at *m/z* 913 ($Y_{3\alpha}^+$) and 1237 ($Y_{3\beta}^+$), which would be predominantly produced from Man7/D1 by the cleavage of the α1–6-linked or α1–3-linked branch arm of the core mannose (Fig. 3A) (nomenclature proposed by Domon and Costello [37]). Likewise, the oligosaccharide at 17 min could be Man7/D3 based on the intensity of Y_{3x}^+ at *m/z* 1075 generated from Man7/D3 by the cleavages of both the α1–6-linked and α1–3-linked branch arms (Fig. 3B).

Fig. 4A and B show the product ion spectra of TetraNA$_4$ in positive and negative ion modes, respectively. In positive ion mode, the characteristic B ions such as *m/z* 454 (B_{2x}^+), 657 (B_{3x}^+), 1475 (B_{4x}^+), and 1658 (B_6^{2+}), and a ladder of several Y ions with intervals corresponding to Hex, HexNAc, and NeuAc were detected. B/Y ions were also detected at *m/z* 366, 527, 819 (B_5/Y_{3x}^{2+}), and 1330 (B_6/Y_{4x}^{2+}). In negative ion mode, only sialic acids were predominantly eliminated by MS^2 and MS^3. The structural information was provided by MS^4, whereby both B and Y ions were originated from TetraNA$_2$, together with the internal fragmentation ions and cross ring cleaved ions (Fig. 4B). In addition to the B and Y ions, which were predominantly produced in positive ion mode, fragment ions at *m/z* 470 ($C_{2x'}^-$), 1322 ($Z_{6x'}^{2-}$, $[Y_{6x'}\text{-}H_2O]^{2-}$), 1241 ($Z_{5x'}^{2-}$, $[Y_{5x'}\text{-}H_2O]^{2-}$), and 1057 ($Y_{5x''}/Z_{4x'}^{2-}$, $Y_{4x'}/Z_{5x''}^{2-}$, $Y_{4x''}/Z_{5x'}^{2-}$, $Y_{5x'}/Z_{4x''}^{2-}$, $[Y_{4x'/5x''}\text{-}H_2O]^{2-}$, $[Y_{4x''/5x'}\text{-}H_2O]^{2-}$) were detected in negative ion mode. These ions were also useful for the structural characterization of oligosaccharides.

3.2. Glycosylation analysis of Thy-1 by GCC-LC/IT-MS-FT-ICR-MS

The improved oligosaccharide profiling using IT–MS-FT–ICR-MS was applied to the glycosylation analysis of Thy-1. PIPLC-treated Thy-1 in rat brain was isolated by SDS-PAGE [31]. N-linked oligosaccharides were extracted from the gel after in-gel PNGase F digestion and were reduced

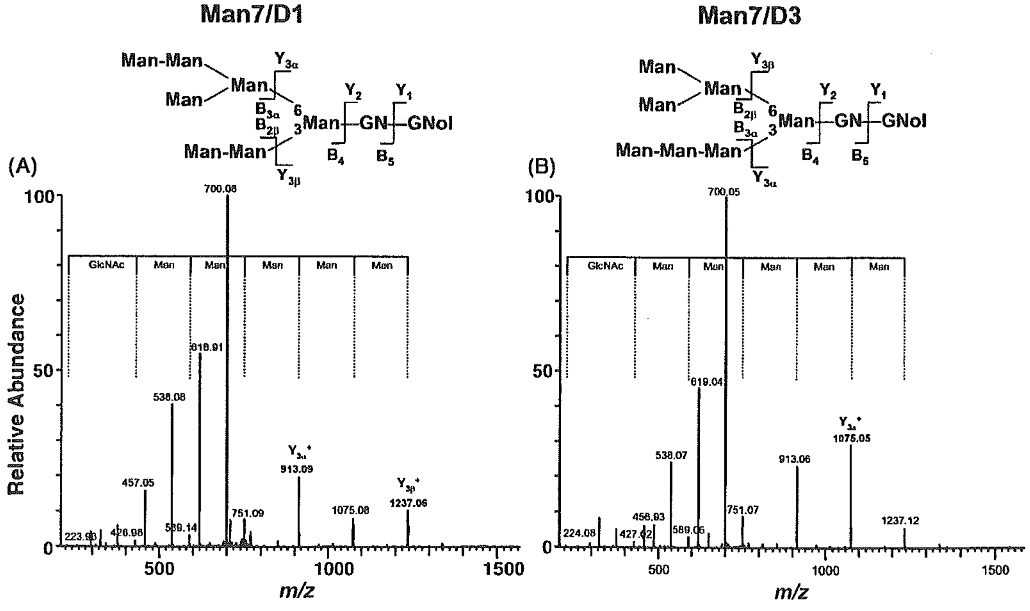

Fig. 3. Product ion spectra of oligosaccharide Man 7/D1 (A) and Man 7/D3 (B).

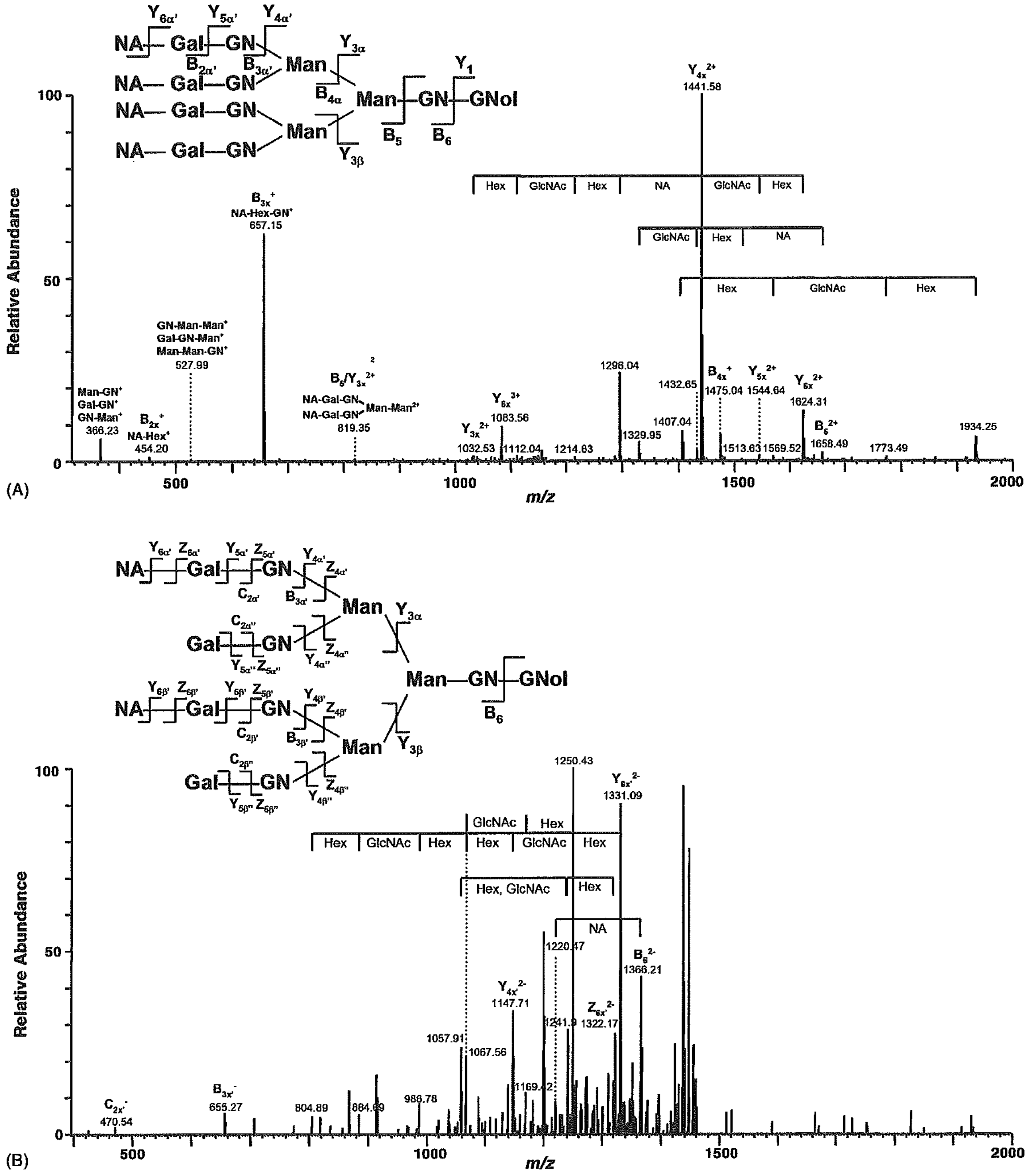

Fig. 4. Product ion spectra of model oligosaccharide, TetraNA$_4$. (A) MS^2 spectrum derived from [TetraNA$_4$]$^{3+}$ at *m/z* 1180 in positive ion mode. (B) MS^4 spectrum derived from [TetraNA$_4$]$^{3-}$ at *m/z* 1178 → [TetraNA$_3$]$^{3-}$ at *m/z* 1081 → [TetraNA$_2$]$^{2-}$ at *m/z* 1476 in negative ion mode.

with NaBH$_4$. Fig. 5 shows total ion chromatogram (TIC) (A) obtained by GCC–LC/IT–MS–FT–ICR–MS of borohydrate-reduced oligosaccharides, and two-dimensional display of full MS^1 scans in positive ion mode (red) and negative ion mode (blue) (B), in which oligosaccharides appear as protonated and ammonium adducted forms along with fragment ions. Alternative scanning in potitive and negative ion mode enables us to detect many oligosaccharides without missing less ionized oligosaccharides in either ion mode. For example, oligosaccharides at *m/z* 762 (2+) and 822 (2+) were detected only in positive ion mode, whereas those at *m/z* 1387 (2−), 1440 (2−), and 1542 (2−) were detected only in negative ion mode. Furthermore, accurate *m/z* values acquired by FT–ICR–MS provide their monosaccharide composition, and subsequent data-dependent MS^n allows us to elucidate their monosaccharide sequence as follows.

3.2.1. Monosaccharide composition of oligosaccharides

Oligosaccharides in Thy-1 were assigned to NeuAc$_{0–3}$ dHex$_{0–3}$Hex$_{3–9}$HexNAc$_{1–5}$HexNAcol$_1$ based on their accurate *m/z* values (Table 1). Oligosaccharides bearing two Fuc residues, in which the *m/z* values of multiple charged ions are nearly identical to those of oligosaccharides bearing one NeuAc residue instead, could be determined

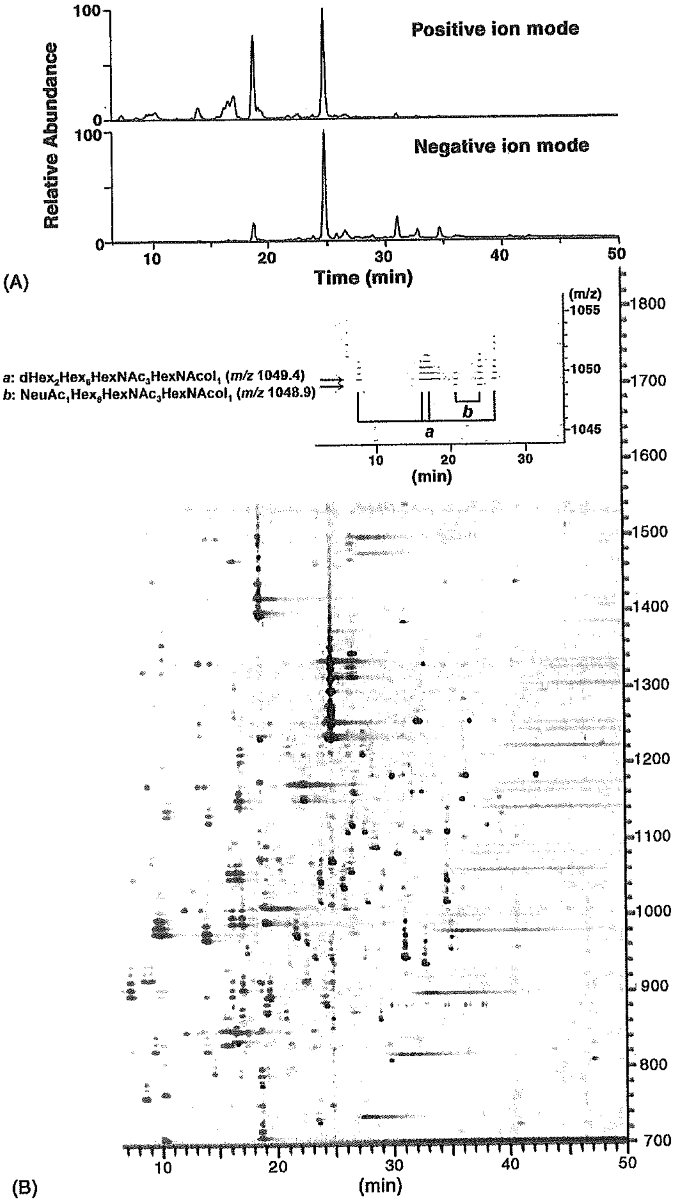

Fig. 5. N-Linked oligosaccharide profile of rat brain Thy-1 obtained by full MS^1 scans with FT–ICR–MS. (A) TIC, and (B) overlapped 2D display in positive (red) and negative (blue) ion modes.

by FT–ICR–MS. For instance, difucosylated oligosaccharides (dHex$_2$Hex$_6$HexNAc$_3$HexNAcol$_1$, theoretical molecular weight: 2096.78 Da) detected at 7.6, 16, 17, and 26 min (Fig. 5, inset, a) were clearly distinguished from monosialylated oligosaccharides (NeuAc$_1$Hex$_6$HexNAc$_3$HexNAcol$_1$, theoretical molecular weight: 2095.76 Da) detected at 21 and 24 min (Fig. 5, inset, b). The improved oligosaccharide profiling indicated that Thy-1 possesses a significant variety of N-linked oligosaccharides containing high-mannose-type (Man5, Man6, Man7, Man8, and M9) and many different complex- and hybrid-type oligosaccharides bearing NeuAc$_{0\text{–}3}$ and Fuc$_{0\text{–}3}$. These results are coincident with those of our previous study, in which we carried out mass spectrometric analysis of Thy-1 glycopeptides.

3.2.2. *Monosaccharide sequence of oligosaccharides*

Monosaccharide sequences of oligosaccharides were elucidated based on the MS/MS spectra. One of the remarkable features of Thy-1 oligosaccharides is the attachment of multiple Fuc and NeuAc residues. We describe below some examples of assignment fucosylated and sialylated oligosaccharides.

3.2.2.1. Gal-(Fuc–)GlcNAc–(Lewis a/x type). Fig. 6A shows the product ion spectrum of a difucosylated oligosaccharide, dHex$_2$Hex$_4$HexNAc$_3$HexNAcol$_1$, at *m/z* 887 (24.3 min) in positive ion mode. There are two possible sites of fucosylation: GlcNAc at the non-reducing end and at the reducing end in the trimannosyl core. The ions detected at *m/z* 350 (Fuc-GlcNAc$^+$, $B_{2\alpha}/Y_{5\alpha'}{}^+$), 370 (Fuc-GlcNAcol$^+$, $Y_{1\alpha}{}^+$), and 512 (Gal-(Fuc–)GlcNAc$^+$, $B_{2\alpha}{}^+$) indicate that Fuc residues link to both the non-reducing end like Lewis a/x, and the inner trimannosyl core GlcNAc. Other ions detected at *m/z* 1553 ($Z_{3\gamma}{}^+$, [$Y_{3\gamma}$-H_2O]$^+$) and 1570 ($Y_{3\gamma}{}^+$) suggest a linkage of non-substituted HexNAc at the terminal end. From these characteristic ions together with a Y ion at *m/z* 938.03 ($Y_{3\alpha/3\beta}{}^+$), it can be deduced that this HexNAc is a bisecting GlcNAc that attaches to the core mannose residue via β1–4 linkage. On the basis of these product ions, the oligosaccharide is assigned to the structure indicated in Fig. 6A, inset.

3.2.2.2. Fuc-Gal-(Fuc–)GlcNAc–(Lewis b/y type). Fig. 6B is the product ion spectrum of a difucosylated oligosaccharide, dHex$_2$Hex$_5$HexNAc$_4$HexNAcol$_1$, at *m/z* 1070 (9.2 min). The characteristic ions at *m/z* 512 (Gal-(Fuc–)GlcNAc$^+$, Fuc-Gal-GlcNAc$^+$, $B_{3\alpha'}/Y_{6\alpha'''}{}^+$, $B_{3\alpha'}/Y_{5\alpha''''}{}^+$) and 1915 ($B_6{}^+$) suggest the absence of Fuc at the reducing end GlcNAc; a B ion at *m/z* 658 ($B_{3\alpha'}{}^+$), a B/Y ion at *m/z* 350, and a Y ion at *m/z* 1408 ($Y_{3\beta/4\alpha''}{}^+$) suggest the attachment of two Fuc to Gal-GlcNAc at the non-reducing end, in a similar manner to the Lewis b/y antigen, Fuc-Gal-(Fuc–)GlcNAc–. A Y ion at *m/z* 1936 ($Y_{4\alpha''}{}^+$) indicates a linkage of non-substituted HexNAc at the terminal end. A B/Y ion at *m/z* 877 ($B_{4\alpha}/Y_{5\alpha''''}{}^+$, $B_{4\alpha}/Y_{6\alpha'''}{}^+$) and a Y ion at *m/z* 1610 ($Y_{3\beta}{}^+$) suggest that this non-substituted HexNAc residue is linked to the mannose residue attached to the Fuc-Gal-(Fuc–)GlcNAc– structure. These ions lead to assignment of this oligosaccharide as the structure indicated in Fig. 6B, inset.

3.2.2.3. NeuAc-Gal-(NeuAc–)GlcNAc–. Fig. 7A shows the product ion spectrum of a disialylated oligosaccharide, NeuAc$_2$dHex$_1$Hex$_5$HexNAc$_2$HexNAcol$_1$, at *m/z* 1085 (30.4 min). Characteristic fragment ions at *m/z* 495 ($B_{3\alpha}/Y_{5\alpha'}{}^+$), 948 ($B_{3\alpha}{}^+$), and 1110 ($B_{4\alpha}{}^+$), together with B ions at *m/z* 453 ($B_{2\alpha'}{}^+$) and 657 ($B_{3\alpha}/Y_{5\alpha''}{}^+$, $B_{3\alpha}/Y_{6\alpha'}{}^+$) suggest the presence of a partial structure of NeuAc-Gal-(NeuAc–)GlcNAc–. Furthermore, detection of Y ions at *m/z* 370 ($Y_{1\alpha}{}^+$) and 1059 ($Y_{3\alpha}{}^+$, $Y_{4\alpha/4\beta}{}^+$) as well as a B ion at *m/z* 1799 ($B_6{}^+$) indicate the linkage of a Fuc residue at the inner trimannosyl core GlcNAc. Based on these product ions, the oligosaccharide detected at *m/z* 1085 was assigned to the structure in Fig. 7A, inset.

Table 1
Summary of N-linked oligosaccharides of rat brain Thy-1

Monosacchardie composition^a				Theoretical mass^b	Positive ion mode		Negative ion mnmode		Deduced structure^d
dHex	Hex	HX	NA		Observed m/z^c	Retention time (min)	Observed m/z^c	Retention time (min)	
1	3	2	0	1058.40	1059.46(1)	29.17			CoreF
0	5	2	0	1236.45	1237.47(1)	24.74	1235.45(1)	24.76	M5
0	3	4	0	1318.50	1319.57(1)	8.63			
0	6	2	0	1398.50	1399.53(1)	18.73	1397.50(1)	18.68	M6
0	5	3	0	1439.53	1440.59(1)	9.17			
1	3	4	0	1464.56	733.31(2), 1465.65(1)	23.44			
0	3	5	0	1521.58	761.80(2)	8.63			BisectGN
0	7	2	0	1560.55	781.29(2), 1561.60(1)	18.66			M7
1	5	3	0	1585.59	793.82(2)	14.59			Hybrid
1	5	3	0	1585.59	793.81(2)	19.13			
1	5	3	0	1585.59	793.83(2)	20.96			
0	5	4	0	1642.61	822.33(2)	9.48			Hybrid
0	5	4	0	1642.61	822.33(2)	14.02			
1	3	5	0	1667.64	834.83(2), 1668.69(1)	16.48	832.81(2)	16.44	CoreF
0	4	5	0	1683.63	842.85(2)	17.48			Hybrid
0	8	2	0	1722.61	870.83(2)^e	17.07			M8
0	5	3	1	1730.62	866.34(2)	20.31			
0	5	3	1	1730.62	866.35(2)	28.91	864.31(2), 1729.64(1)	28.93	Hybrid
2	5	3	0	1731.64	866.86(2)	20.83	864.81(2)	20.85	Hybrid, CoreF, Lax
1	6	3	0	1747.64	874.84(2)	19.19			
2	4	4	0	1772.67	887.37(2)	23.84	885.33(2)	23.86	
2	4	4	0	1772.67	887.36(2)	24.25	885.33(2)	24.27	Hybrid, CoreF, BisectGN
1	5	4	0	1788.67	895.36(2)	7.37			Hybrid
1	5	4	0	1788.67	895.36(2)	13.90			
1	5	4	0	1788.67	895.35(2)	14.16			Hybrid, CoreF
1	5	4	0	1788.67	895.35(2)	19.44	893.33(2)	19.46	Hybrid, CoreF
0	6	4	0	1804.66	903.35(2)	17.07	901.33(2)	17.09	Hybrid, BisectGN
1	4	5	0	1829.69	915.88(2)	8.63			Hybrid
1	4	5	0	1829.69	915.88(2)	9.17			Hybrid
1	4	5	0	1829.69	915.89(2)	18.00			Hybrid
1	4	5	0	1829.69	915.89(2)	22.61	913.84(2)	22.63	
1	5	3	1	1876.68	939.37(2)	21.17	937.34(2)	21.12	
1	5	3	1	1876.68	939.36(2)	24.90	937.34(2)	24.92	
1	5	3	1	1876.68	939.39(2)	32.76	937.33(2)	32.78	Hybrid, CoreF
0	9	2	0	1884.66	951.88(2)^e	17.53			M9
0	6	3	1	1892.68	947.39(2)	23.31	945.33(2)	23.33	Hybrid
0	6	3	1	1892.68	947.39(2)	31.09	945.33(2)	31.05	Hybrid
2	6	3	0	1893.70	947.87(2)	24.61	945.84(2)	24.70	
1	4	4	1	1917.71			957.85(2)	27.73	
1	4	4	1	1917.71			957.85(2)	28.86	
1	4	4	1	1917.71			957.85(2)	34.91	CoreF
1	4	4	1	1917.71			957.85(2)	35.55	
0	5	4	1	1933.70	967.89(2)	22.61	965.85(2)	22.63	Hybrid
0	5	4	1	1933.70	967.86(2)	24.61	965.82(2)	24.70	
2	5	4	0	1934.72	968.39(2)	13.97			Hybrid
1	6	4	0	1950.72	976.39(2)	9.93			Hybrid, Lax
1	6	4	0	1950.72	976.41(2)	21.76	974.35(2)	21.79	Hybrid, CoreF
2	4	5	0	1975.75	988.90(2)	16.21	986.85(2)	16.16	Complex
2	4	5	0	1975.75	988.90(2)	17.07	986.87(2)	17.09	Complex
0	5	3	2	2021.72			1009.86(2)	26.35	
0	5	3	2	2021.72			1009.85(2)	26.83	
1	6	3	1	2038.73	1020.40(2)	23.84	1018.36(2)	23.80	
1	6	3	1	2038.73	1020.44(2)	27.77	1018.37(2)	27.80	CoreF
1	6	3	1	2038.73	1020.42(2)	34.66	1018.36(2)	34.69	Hybrid, CoreF
1	5	4	1	2079.76	1040.92(2)	25.73	1038.87(2)	25.81	CoreF
1	5	4	1	2079.76	1040.92(2)	29.04	1038.88(2)	28.99	
3	5	4	0	2080.78	1041.42(2)	23.84	1039.39(2)	23.86	
0	6	4	1	2095.76	1048.94(2)	20.57			Hybrid
0	6	4	1	2095.76	1048.91(2)	23.84	1046.87(2)	23.80	Hybrid
2	6	4	0	2096.78	1049.42(2)	7.58			

Table 1 (*Continued*)

Monosacchardie composition[a]				Theoretical mass[b]	Positive ion mode		Negative ion mnmode		Deduced structure[d]
dHex	Hex	HX	NA		Observed *m*/*z*[c]	Retention time (min)	Observed *m*/*z*[c]	Retention time (min)	
2	6	4	0	2096.78	1049.42(2)	15.97			
2	6	4	0	2096.78	1049.42(2)	16.61			Hybrid, BisectGN
2	6	4	0	2096.78	1049.43(2)	25.73			
1	7	4	0	2112.77			1055.38(2)	34.62	
1	4	5	1	2120.79	1061.45(2)	20.43			Complex
1	4	5	1	2120.79	1061.45(2)	24.74	1059.39(2)	24.70	
1	4	5	1	2120.79	1061.45(2)	26.47	1059.39(2)	26.42	CoreF
2	5	5	0	2137.80	1069.94(2)	9.17			Lby
2	5	5	0	2137.80	1069.94(2)	21.30			
2	5	5	0	2137.80	1069.95(2)	23.09	1067.9(2)	23.04	
1	5	3	2	2167.78	1084.94(2)	30.41	1082.89(2)	30.37	Hybrid, CoreF
2	4	6	0	2178.83	1090.45(2)	26.08			
0	6	3	2	2183.77	1092.95(2)	28.63	1090.88(2)	28.60	Hybrid, diSia
0	5	4	2	2224.80	1113.45(2)	26.10			
2	5	4	1	2225.82	1113.95(2)	27.56			
2	5	4	1	2225.82	1113.98(2)	34.80			
1	6	4	1	2241.81	1121.95(2)	26.60	1119.90(2)	26.63	
1	6	4	1	2241.81			1119.90(2)	30.58	
1	6	4	1	2241.81			1119.91(2)	38.14	
3	6	4	0	2242.83	1122.46(2)	14.23			
2	7	4	0	2258.83	1130.46(2)	10.47			
3	5	5	0	2283.86	1142.96(2)	16.87			
1	4	6	1	2323.87	1162.98(2)	26.60			
1	6	3	2	2329.83			1163.91(2)	31.72	
1	6	3	2	2329.83			1163.91(2)	32.54	Hybrid, diSia
1	5	4	2	2370.86	1186.55(2)	29.89	1184.42(2)	30.00	Complex, CoreF
1	5	4	2	2370.86			1184.43(2)	36.00	
1	5	4	2	2370.86	1186.52(2)	36.31	1184.42(2)	36.40	Complex, CoreF
1	5	4	2	2370.86	1186.50(2)	42.47	1184.43(2)	42.43	Complex, CoreF
3	5	4	1	2370.86			1184.93(2)	30.99	
2	5	5	1	2428.90	1215.50(2)	21.17	1213.44(2)	21.25	
2	5	5	1	2428.90	1215.50(2)	23.84			
2	5	5	1	2428.90	1215.52(2)	26.32	1213.45(2)	26.28	
2	5	5	1	2428.90	1215.50(2)	27.50	1213.45(2)	27.53	
2	5	4	2	2516.91	1259.60(2)	32.23	1257.45(2)	32.19	Complex, Lax, CoreF, diSia
2	5	4	2	2516.91			1257.45(2)	36.72	
2	5	6	1	2631.98			876.32(3), 1314.99(2)	26.76	
3	5	4	2	2662.97			1330.49(2)	32.78	
1	5	6	2	2777.02			1387.50(2)	30.99	
0	6	5	3	2881.03			1439.50(2)	34.83	
0	6	5	3	2881.03			1439.49(2)	40.77	
2	6	5	2	2882.05			1440.05(2)	37.96	
2	6	6	2	3085.13			1541.55(2)	31.38	

[a] dHex, deoxyhexose; Hex, hexose; HX, *N*-acetylhexamine; NeuAc, *N*-acetylneuramic acid.

[b] Monoisotopic value.

[c] Values in parentheses are charge state.

[d] Structures are deduced by MS^n. Complex, complex-type-oligosaccharide; Hybrid, hybrid-type-oligosaccharide; M5-9, high-mannose-type oligosccharide containing 5–9 mannose residues; BisectGN, bisecting GlcNAc; Lax, Lewis a/x structure; Lby, Lewis b/y structure; diSia, disialic acid.

[e] Ammonium adducted form.

3.2.2.4. NeuAc-Gal-GlcNAc—. Fig. 7B shows the product ion spectrum of a disialylated oligosaccharide, $NeuAc_2dHex_1Hex_5HexNAc_3HexNAcol_1$, at *m*/*z* 1187 (42.5 min). Although B ions were detected at *m*/*z* 454 (B_{2x}^+), 657 (B_{3x}^+) and 819 (B_{4x}^+), none of the fragment ions at *m*/*z* 495 (NeuAc-GlcNAc$^+$), 948 (NeuAc-Gal-(NeuAc—)GlcNAc$^+$), or 1110 (NeuAc-Gal-(NeuAc—)GlcNAc-Man$^+$) were detected in the spectrum. This result suggests that the two NeuAc residues occupy both non-reducing ends of the biantennary form. Fucosylation of the inner trimannnosyl core GlcNAc was determined by the detection of Y ions at *m*/*z* 370 ($Y_{1\alpha}^+$) and 1059 ($Y_{4\alpha/4\beta}^+$). These product ions lead to assignment of this oligosaccharide the structure in Fig. 6B.

3.2.2.5. (v) NeuAc-NeuAc—. Fig. 7C shows the product ion spectrum of a disialylated and difucosylated oligosaccharide, $NeuAc_2dHex_2Hex_5HexNAc_3HexNAcol_1$, at *m*/*z* 1260 (32.2 min). The characteristic ions at *m*/*z* 583 (NeuAc-NeuAc$^+$,

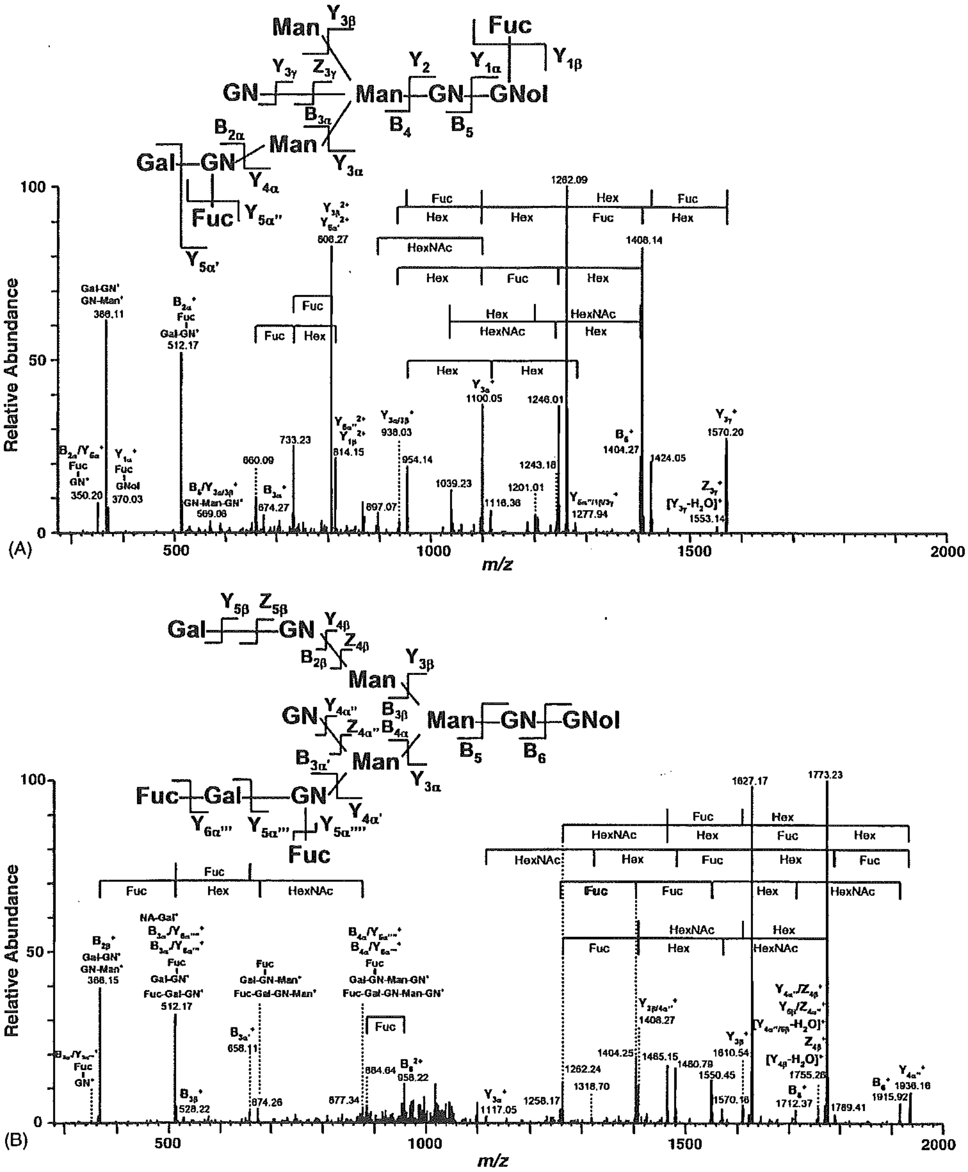

Fig. 6. Product ion spectra of N-linked oligosaccharides of rat brain Thy-1. (A) MS^2 spectrum of dHex$_2$Hex$_4$HexNAc$_3$HexNAcol$_1$ at *m/z* 887 (24.3 min). (B) MS^2 spectrum of dHex$_2$Hex$_5$HexNAc$_4$HexNAcol$_1$ at *m/z* 1070 (9.2 min).

$B_{2\alpha'}{}^{+}$), 949 (NeuAc-NeuAc-Gal-GlcNAc$^+$, $B_{3\alpha}/Y_{5\alpha''}{}^{+}$), and 1094 (NeuAc-NeuAc-Gal-(Fuc−)GlcNAc$^+$, $B_{3\alpha}{}^{+}$) suggest that this oligosaccharide contains a disialic acid residue and one Fuc at the non-reducing end. In addition, a Y ion at *m/z* 370 ($Y_{1\alpha}{}^{+}$) indicated that the other Fuc was attached to GlcNAc at the reducing end. Based on these product ions, this oligosaccharide structure could be assigned as indicated in Fig. 7C, inset.

4. Discussion

Thy-1 has three *N*-glycosylation sites, Asn23, 74, and 98. We have previously demonstrated the attachment of high-mannose-type, complex-type, and hybrid-type oligosaccharides to these sites. Asn74 is occupied with various *N*-glycans, which have been estimated to be fucosylated and sialylated [31]. Product ion spectra containing fucosylation and sialylation isomers make it difficult to elucidate the detailed structure. We have conducted mass spectrometric oligosaccharide analysis through the separation of diverse oligosaccharides with GCC. We first improved the mass spectrometric oligosaccharide profiling by IT–MS-FT–ICR–MS. The improved method enabled the monosaccharide composition analysis and sequencing of both neutral and acidic oligosaccharides in a single run. Using this method, we successfully analyzed various *N*-glycans of Thy-1 that could not be characterized by the analysis of glycopeptides. We found a Lewis b/y structure and sialylated GlcNAc in the branch structure. Interestingly, disialic acid (NeuAc-NeuAc−), which is known to be involved in neurite formation was found in brain Thy-1 [38].

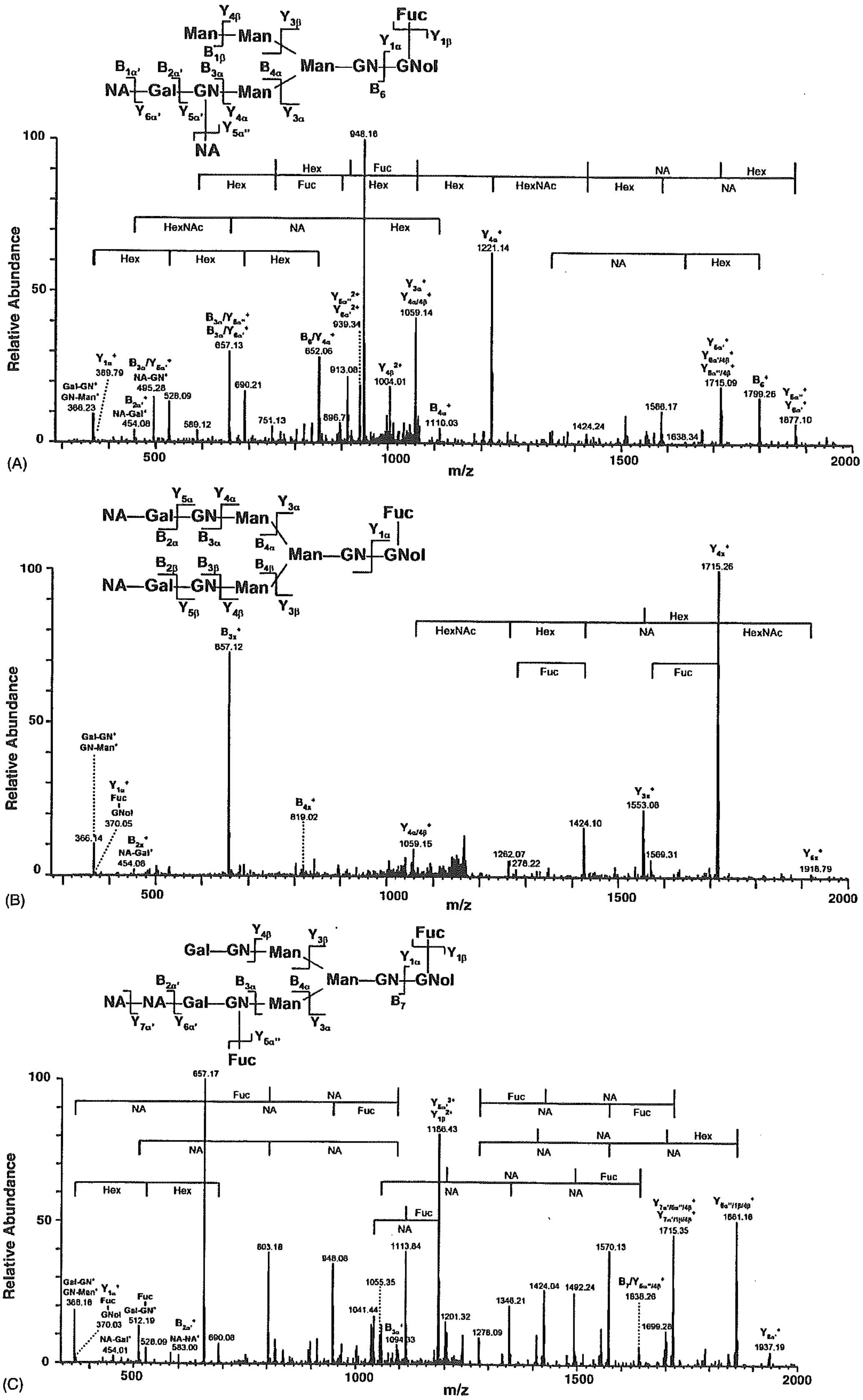

Fig. 7. Product ion spectra of N-linked oligosaccharides of rat brain Thy-1. (A) MS^2 spectrum of NeuAc$_2$dHex$_1$Hex$_5$HexNAc$_2$HexNAcol$_1$ at *m/z* 1085 (30.4 min). (B) MS^2 spectrum of NeuAc$_2$dHex$_1$Hex$_5$HexNAc$_3$HexNAcol$_1$ at *m/z* 1187 (42.5 min). (C) MS^2 spectrum of NeuAc$_2$dHex$_2$Hex$_5$HexNAc$_3$HexNAcol$_1$ at *m/z* 1260 (32.2 min).

In these two studies, we have demonstrated a strategy for glycosylation analysis of Thy-1, including identification of a glycoprotein, determination of glycosylation sites, site-specific glycosylation analysis, and structural analysis of oligosaccharide details. This strategy can be applied to glycosylation analysis of other glycoproteins. Specifically, the glycoprotein sample is divided into two. One is subjected to proteinase digestion followed by peptide/glycopeptide mapping, which provides information on glycosylation sites and site-specific heterogeneity. The other is subjected to PNGase F digestion followed by mass spectrometric oligosaccharide profiling, by which a detailed structure of *N*-glycans released from a glycoprotein could be provided. Recently, proteomic approaches, which are based on two-dimensional electrophoresis followed by mass spectrometry, have been used in various fields. Although glycosylation analysis of abundant glycoproteins in gel has been successful, that of a low-abundance glycoprotein in gel remains a great challenge. The proposed method consisting of peptide/glycopeptide mapping followed by oligosaccharide profiling with sequential scans by IT–MS-FT–ICR–MS will likely be a powerful tool for glycosylation analysis of low-abundance glycoproteins and for proteomics/glycomics.

Acknowledgements

This work was supported in part by a Grant-in-Aid for Creative Scientific Research (16GS0313) from the Ministry of Education, Culture, Sports, and Technology, the Ministry of Health, Labor and Welfare, and Core Research for the Evolutional Science and Technology Program (CREST) of the Japan Science and Technology Agency (JST).

We appreciate Dr. A. Hachisuka of the National Institute of Health Science for her technical advice.

We thank Dr. M. Kubota and Mr. M. Yoshida of Thermo Electron K.K. (Japan) for their technical support.

References

[1] A. Varki, Glycobiology 3 (1993) 97.
[2] J.W. Dennis, M. Granovsky, C.E. Warren, Biochim. Biophys. Acta 1473 (1999) 21.
[3] Y. Sato, M. Kimura, C. Yasuda, Y. Nakano, M. Tomita, A. Kobata, T. Endo, Glycobiology 9 (1999) 655.
[4] G. Durand, N. Seta, Clin. Chem. 46 (2000) 795.
[5] O. Krokhin, W. Ens, K.G. Standing, J. Wilkins, H. Perreault, Rapid Commun. Mass Spectrom. 18 (2004) 2020.
[6] Y. Satomi, Y. Shimonishi, T. Takao, FEBS Lett. 576 (2004) 51.
[7] Y. Wada, M. Tajiri, S. Yoshida, Anal. Chem. 76 (2004) 6560.
[8] W. Chai, V. Piskarev, A.M. Lawson, Anal. Chem. 73 (2001) 651.
[9] D. Sagi, J. Peter-Katalinic, H.S. Conradt, M. Nimtz, J. Am. Soc. Mass Spectrom. 13 (2002) 1138.
[10] A. Zamfir, D.G. Seidler, H. Kresse, J. Peter-Katalinic, Glycobiology 13 (2003) 733.
[11] D.J. Harvey, R.L. Martin, K.A. Jackson, C.W. Sutton, Rapid Commun. Mass Spectrom. 18 (2004) 2997.
[12] C. Robbe, C. Capon, B. Coddeville, J.C. Michalski, Rapid Commun. Mass Spectrom. 18 (2004) 412.
[13] N. Ojima, K. Masuda, K. Tanaka, O. Nishimura, J. Mass Spectrom. 40 (2005) 380.
[14] C.W. Sutton, J.A. O'Neill, J.S. Cottrell, Anal. Biochem. 218 (1994) 34.
[15] B. Küster, S.F. Wheeler, A.P. Hunter, R.A. Dwek, D.J. Harvey, Anal. Biochem. 250 (1997) 82.
[16] B. Küster, T.N. Krogh, E. Mortz, D.J. Harvey, Proteomics 1 (2001) 350.
[17] K. Hirayama, R. Yuji, N. Yamada, K. Kato, Y. Arata, I. Shimada, Anal. Chem. 70 (1998) 2718.
[18] F. Wang, A. Nakouzi, R.H. Angeletti, A. Casadevall, Anal. Biochem. 314 (2003) 266.
[19] K. Sandra, I. Stals, P. Sandra, M. Claeyssens, J. Van Beeumen, B. Devreese, J. Chromatogr. A 1058 (2004) 263.
[20] Y. Satomi, Y. Shimonishi, T. Hase, T. Takao, Rapid Commun. Mass Spectrom. 18 (2004) 2983.
[21] A. Harazono, N. Kawasaki, T. Kawanishi, T. Hayakawa, Glycobiology 15 (2005) 447.
[22] M. Wuhrer, C.A. Koeleman, C.H. Hokke, A.M. Deelder, Anal. Chem. 77 (2005) 886.
[23] B.L. Schulz, N.H. Packer, N.G. Karlsson, Anal. Chem. 74 (2002) 6088.
[24] N.L. Wilson, B.L. Schulz, N.G. Karlsson, N.H. Packer, J. Proteome Res. 1 (2002) 521.
[25] L.A. Gennaro, D.J. Harvey, P. Vouros, Rapid Commun. Mass Spectrom. 17 (2003) 1528.
[26] N.G. Karlsson, B.L. Schulz, N.H. Packer, J. Am. Soc. Mass Spectrom. 15 (2004) 659.
[27] N.G. Karlsson, N.L. Wilson, H.J. Wirth, P. Dawes, H. Joshi, N.H. Packer, Rapid Commun. Mass Spectrom. 18 (2004) 2282.
[28] M. Wuhrer, C.A. Koeleman, A.M. Deelder, C.H. Hokke, Anal. Chem. 76 (2004) 833.
[29] Y. Takegawa, K. Deguchi, S. Ito, S. Yoshioka, H. Nakagawa, S. Nishimura, Anal. Chem. 77 (2005) 2097.
[30] S. Itoh, N. Kawasaki, M. Ohta, T. Hayakawa, J. Chromatogr. A 978 (2002) 141.
[31] S. Itoh, N. Kawasaki, A. Harazono, N. Hashii, Y. Matsuishi, T. Kawanishi, T. Hayakawa, J. Chromatogr. A 1094 (2005) 105.
[32] N. Kawasaki, M. Ohta, S. Hyuga, O. Hashimoto, T. Hayakawa, Anal. Biochem. 269 (1999) 297.
[33] S. Itoh, N. Kawasaki, M. Ohta, M. Hyuga, S. Hyuga, T. Hayakawa, J. Chromatogr. A 968 (2002) 89.
[34] N. Kawasaki, S. Itoh, M. Ohta, T. Hayakawa, Anal. Biochem. 316 (2003) 15.
[35] C. Bordier, J. Biol. Chem. 256 (1981) 1604.
[36] M.P. Lisanti, M. Sargiacomo, L. Graeve, A.R. Saltiel, E. Rodriguez-Boulan, Proc. Natl. Acad. Sci. U.S.A. 85 (1988) 9557.
[37] B. Domon, C.E. Costello, Glycoconjugate J. 5 (1988) 397.
[38] C. Sato, T. Matsuda, K. Kitajima, J. Biol. Chem. 277 (2002) 45299.

ELSEVIER

Available online at www.sciencedirect.com

SCIENCE DIRECT®

Analytical Biochemistry 348 (2006) 259–268

ANALYTICAL
BIOCHEMISTRY

www.elsevier.com/locate/yabio

Site-specific N-glycosylation analysis of human plasma ceruloplasmin using liquid chromatography with electrospray ionization tandem mass spectrometry

Akira Harazono *, Nana Kawasaki, Satsuki Itoh, Noritaka Hashii,
Akiko Ishii-Watabe, Toru Kawanishi, Takao Hayakawa

National Institute of Health Sciences, Division of Biological Chemistry and Biologicals, 1-18-1 Kami-yoga, Setagaya-Ku, Tokyo 158-8501, Japan

Received 8 June 2005
Available online 10 November 2005

Abstract

Ceruloplasmin has ferroxidase activity and plays an essential role in iron metabolism. In this study, a site-specific glycosylation analysis of human ceruloplasmin (CP) was carried out using reversed-phase high-performance liquid chromatography with electrospray ionization tandem mass spectrometry (LC-ESI-MS/MS). A tryptic digest of carboxymethylated CP was subjected to LC-ESI-MS/MS. Product ion spectra acquired data-dependently were used for both distinction of the glycopeptides from the peptides using the carbohydrate B-ions, such as *m/z* 204 (HexNAc) and *m/z* 366 (HexHexNAc), and identification of the peptide moiety of the glycopeptide based on the presence of the b- and y-series ions derived from the peptide. Oligosaccharide composition was deduced from the molecular weight calculated from the observed mass of the glycopeptide and theoretical mass of the peptide. Of the seven potential N-glycosylation sites, four (Asn119, Asn339, Asn378, and Asn743) were occupied by a sialylated biantennary or triantennary oligosaccharide with fucose residues (0, 1, or 2). A small amount of sialylated tetraantennary oligosaccharide was detected. Exoglycosidase digestion suggested that fucose residues were linked to reducing end GlcNAc in biantennary oligosaccharides and to reducing end and/or α1–3 to outer arms GlcNAc in triantennary oligosaccharides and that roughly one of the antennas in triantennary oligosaccharides was α2–3 sialylated and occasionally α1–3 fucosylated at GlcNAc.

© 2005 Elsevier Inc. All rights reserved.

Keywords: Ceruloplasmin; Glycopeptide; Liquid chromatography-electrospray tandem mass spectrometry; Product ion spectrum; Exoglycosidase digestion

Ceruloplasmin (CP)[1] is a blue copper serum glycoprotein synthesized in the liver. CP has ferroxidase activity and plays an essential role in iron metabolism [1–4]. The primary structure of human CP has been determined by amino acid sequencing, and it is composed of a single polypeptide chain of 1046 amino acid residues [5]. The amino acid sequence was confirmed from complete cDNA sequence [6]. The major oligosaccharides in human CP were reported to be sialylated bi- and triantennary structures with or without a fucose residue [7,8]. Although four N-glycosylation sites (Asn119, Asn339, Asn378, and Asn743) were identified among seven potential sites [9], the heterogeneity of oligosaccharides was still unknown at each glycosylation site. CP is an acute phase reactant, and the serum concentration increases during inflammation, infection, and trauma [10]. It is known that the patterns of glycosylation are changed by inflammatory cytokines [11]. Several studies have reported that CP is a good diagnostic marker of solid malignant tumors [12,13] and that the CP glycoform might

---

* Corresponding author. Fax: +81 3 3700 9084.
E-mail address: harazono@nihs.go.jp (A. Harazono).

[1] *Abbreviations used:* CP, ceruloplasmin; LC-ESI-MS, liquid chromatography with electrospray ionization mass spectrometry; Hex, hexose; HexNAc, *N*-acetylhexosamine; LC-ESI-MS/MS, liquid chromatography with electrospray ionization tandem mass spectrometry; EDTA, ethylenediaminetetraacetic acid; TFA, trifluoroacetic acid; Q-TOF, quadrupole time-of-flight; TIC, total ion chromatogram; NeuAc, *N*-acetylneuraminic acid; GlcNAc, *N*-acetylglucosamine; Fuc, fucose.

0003-2697/$ - see front matter © 2005 Elsevier Inc. All rights reserved.
doi:10.1016/j.ab.2005.10.036

be a valuable supplement [12]. Thus, it is important to conduct a site-specific glycosylation analysis of normal human CP.

One of the most effective techniques for determining the site-specific carbohydrate heterogeneity of glycoproteins is the mass spectrometric peptide mapping of proteolytic fragments of glycoproteins by liquid chromatography with electrospray ionization mass spectrometry (LC-ESI-MS) [14–19]. The specific detection of glycopeptides in a complex peptide mixture is generally achieved by monitoring specific carbohydrate fragment ions such as *m/z* 204 (HexNAc) and *m/z* 366 (HexHexNAc) produced by cone voltage fragmentation or by precursor ion scanning [15–19]. Because product ion spectra of glycopeptides show high abundant carbohydrate fragment ions and low abundant b- and y-series fragment ions derived from the peptide backbone [20,21], product ion spectra acquired data-dependently in liquid chromatography with electrospray ionization tandem mass spectrometry (LC-ESI-MS/MS) can be used for both the selection from the peptides and the identification of the glycopeptides [22]. MS in combination with specific exoglycosidase digestions allows us to obtain the site-specific information on anomericity and linkage of glycans [23]. In the current study, we conducted a site-specific glycosylation analysis of human CP and successfully determined glycosylation status and glycosylation profile at each N-glycosylation site.

Materials and methods

Materials

Acetonitrile, formic acid, and guanidine hydrochloride were purchased from Wako Pure Chemicals Industries (Osaka, Japan). Purified human CP was purchased from Calbiochem (San Diego, CA, USA). Modified trypsin was purchased from Promega (Madison, WI, USA). α2–3 Neuraminidase (EC 3.2.1.18) of *Macrobdella decora*, a recombinant form, and α1–3,4 fucosidase (EC 3.2.1.51) from *Xanthomonas* sp. were purchased from Calbiochem. α2–3,6,8,9 Neuraminidase (EC 3.2.1.18) of *Arthrobacter ureafaciens*, a recombinant form, and β1–4 galactosidase (EC 3.2.1.23) were purchased from Sigma Chemical (St. Louis, MO, USA). The water used was obtained from a Milli-Q water system (Millipore, Bedford, MA, USA). All other reagents were of the highest quality available.

Reduction and S-carboxymethylation of CP

CP (100 μg) was dissolved in 270 μl of 0.5 M Tris–HCl buffer (pH 8.5) that contained 8 M guanidine hydrochloride and 5 mM ethylenediaminetetraacetic acid (EDTA). After the addition of 2 μl of 2-mercaptoethanol, the mixture was incubated for 2 h at 40 °C. Then 5.67 mg of monoiodoacetic acid was added, and the resulting mixture was incubated for 2 h at 40 °C in the dark. The reaction mixture was applied to a PD-10 column (Amersham Biosciences, Uppsala, Sweden) to remove the reagents, and the eluate was lyophilized.

Trypsin digestion of CP

Reduced and carboxymethylated CP was redissolved in 100 μl of 0.1 M Tris–HCl buffer (pH 8.0). An aliquot of 1 μl of trypsin prepared as 1 μg/μl was added to 50 μl of CP solution (1:50, w/w), and the mixture was incubated for 16 h at 37 °C. The enzyme digestion was stopped by storing at −20 °C before analysis.

HPLC of tryptic digest of CP

Tryptic digests (0.2 and 0.4 μg) of human CP were analyzed by LC-ESI-MS/MS to identify the peptides and glycopeptides, respectively. HPLC was performed on a Paradigm MS 4 (Michrome BioResources, Auburn, CA, USA) equipped with a Magic C18 column (0.2 μ, 50 mm, Michrome BioResources). The eluents consisted of water containing 2% (v/v) acetonitrile and 0.1% (v/v) formic acid (pump A) and 90% acetonitrile and 0.1% formic acid (pump B). Trypsin-digested samples were loaded onto a microtrap (peptide captrap, Michrom BioResources). After a wash with 15 μl H_2O/CH_3CN (98:2) with 0.1% trifluoroacetic acid (TFA), the trapping column was switched into line with the column. Samples were eluted with 5% of B for 10 min, followed by a linear gradient from 5 to 65% of B in 60 min at a flow rate of 2 μl/min.

ESI-Q-TOF-MS/MS

Mass spectrometric analyses were performed using a quadrupole time-of-flight (Q-TOF) mass spectrometer (QSTAR Pulsar, MDS Sciex, Toronto, Canada) equipped with a nano-electrospray ion source. The mass spectrometer was operated in the positive ion mode. The nanospray voltage was set at 2500 V. Mass spectra were acquired at *m/z* 400–2000 or *m/z* 1000–2000 for MS analysis and at *m/z* 100–2000 for MS/MS analysis. After every regular MS acquisition, two MS/MS acquisitions against top two of the multiply charged molecular ions were performed (data-dependent acquisition). The precursor ions with the same *m/z* as acquired previously were excluded for 120 s. The collision energy was varied between 30 and 80 eV depending on the size and charge of the molecular ion. Accumulation times for the spectra were 1.0 and 2.0 s for MS and MS/MS, respectively. All peaks were resolved monoisotopically.

Tandem MS/MS data from LC-ESI-MS/MS runs were submitted to the search engine Mascot to identify the tryptic peptides of CP. One missed cleavage was allowed, and tolerances of 2.0 and 0.8 u mass were used for precursor and product ions, respectively. From the data for LC-ESI-MS/MS at *m/z* 1000–2000, glycopeptide precursor ions were selected manually based on the presence of oligosaccharide oxonium ions such as *m/z* 204 (HexNAc) and *m/z* 366 (HexHexNAc). The glycopeptide ions were assigned based on the presence of b- and y-series fragment ions of peptides of putative glycopeptides or molecular weight difference of sugar unit. The molecular weight of the carbohydrate in the glycopeptide was calculated from the molecular weights of the glycopeptide and the suggested peptide. The oligosaccharide composition and type were deduced from the molecular weight of the carbohydrate.

Oligosaccharide sequencing by exoglycosidase digestions

Trypsin in the digest of human CP was inactivated by boiling for 5 min at 100 °C. Aliquots of the digest (4 μg) were digested in a volume of 20 μl for 12 h at 37 °C in 50 mM sodium phosphate buffer (pH 5.0) using the following exoglycosidases alone or in combination: α2–3 neuraminidase, 20 mU/ml; α2–3,6,8,9 neuraminidase, 100 mU/ml; α1–3,4 fucosidase, 20 mU/ml; and β1–4 galactosidase, 30 mU/ml. Aliquots (0.08 μg) before and after exoglycosidase digestions were subjected to LC-ESI-MS at *m/z* 700 to 2000 in which MS/MS acquisition was not performed.

Results

Peptide mapping of tryptic digest of human CP (LC-ESI-MS/MS in m/z range of 400–2000)

The amino acid sequence of human CP (National Center for Biotechnology Information protein database: P00450) is shown in Fig. 1. The tryptic peptides, including potential N-glycosylation sites, are shown in bold type. Trypsin can digest human CP into seven glycopeptides containing only one potential N-glycosylation site. To determine the glycosylation state at each glycosylation site, we performed mass spectrometric peptide mapping of the tryptic digest of CP. An aliquot of 0.2 μg of the tryptic digest was analyzed by LC-ESI-MS/MS in the *m/z* range of 400–2000 (data not shown). When molecular ions with more than a single charge were detected, the product ion spectrum was acquired automatically. Peptide identification of each product ion spectrum was done using the Mascot search engine. More than 70% of the amino acid sequence was identified; identified amino acids of CP are underlined in Fig. 1. Three peptides containing the potential N-glycosylation site (Asn208, Asn569, and Asn907 [residues 197–218, 558–579, and 895–917, respectively]) were detected, whereas peptides containing the other N-glycosylation sites were not detected. Thus, Asn119, Asn339, Asn378, and Asn743 might be glycosylated.

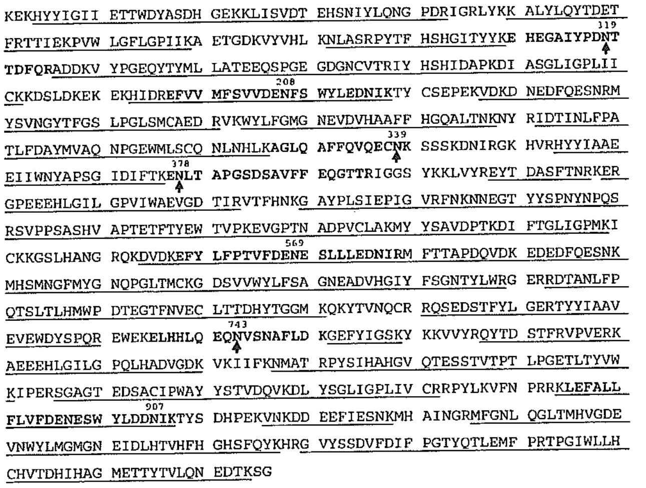

KEKHYYIGII ETTWDYASDH GEKKLISVDT EHSNIYLQNG PDRIGRLYKK ALYLQYTDET
FRTTIEKPVW LGFLGPIIKA ETGDKVYVHL KNLASRPYTF HSHGITYYKE **HEGAIYPDNT**
TDFQRADDKV YPGEQYTYML LATEEQSPGE GDGNCVTRIY HSHIDAPKDI ASGLIGPLII
CKKDSLDKEK EKHIDR**EFVV MFSVVDENFS WYLEDNIK**TY CSEPEKVDKD NEDFQESNRM
YSVNGYTFGS LPGLSMCAED RVKWYLFGMG NEVDVHAAFF HGQALTNKNY RIDTINLFPA
TLFDAYMVAQ NPGEWMLSCQ NLNHLK**AGLQ AFFQVQECNK** SSSKDNIRGK HVRHYYIAAE
EIIWNYAPSG IDIFTK**ENLT APGSDSAVFF EQGTTR**IGGS YKKLVYREYT DASFTNRKER
GPEEEHLGIL GPVIWAEVGD TIRVTFHNKG AYPLSIEPIG VRFNKNNEGT YYSPNYNPQS
RSVPPSASHV APTETFTYEW TVPKEVGPTN ADPVCLAKMY YSAVDPTKDI FTGLIGPMKI
CKKGSLHANG RQKDVDK**EFY LFPTVFDENE SLLLEDNIR**M FTTAPDQVDK EDEDFQESNK
MHSMNGFMYG NQPGLTMCKG DSVVWYLFSA GNEADVHGIY FSGNTYLWRG ERRDTANLFP
QTSLTLHMWP DTEGTFNVEC LTTDHYTGGM KQKYTVNQCR RQSEDSTFYL GERTYYIAAV
EVEWDYSPQR EWEK**ELHHLQ EQNVSNAFLD K**GEFYIGSKY KKVVYRQYTD STFRVPVERK
AEEEHLGILG PQLHADVGDK VKIIFKNMAT RPYSIHAHGV QTESSTVTPT LPGETLTYVW
KIPERSGAGT EDSACIPWAY YSTVDQVKDL YSGLIGPLIV CRRPYLKVFN PRRK**LEFALL**
FLVFDENESW YLDDNIKTYS DHPEKVNKDD EEFIESNKMH AINGRMFGNL QGLTMHVGDE
VNWYLMGMGN EIDLHTVHFH GHSFQYKHRG VYSSDVFDIF PGTYQTLEMF PRTPGIWLLH
CHVTDHIHAG METTYTVLQN EDTKSG

Fig. 1. Primary amino acid sequence of human CP (P00450). The tryptic peptides, including potential N-glycosylation sites, are shown in bold type. Tryptic peptides identified in the LC-ESI-MS/MS analysis are underlined. Cysteine residues are carboxymethylated. Identified N-glycosylation sites are indicated by arrow.

Glycosylation analysis of human CP (LC-ESI-MS/MS in the m/z range of 1000–2000)

N-glycosylated peptides have relatively high molecular weights due to their oligosaccharide moiety. Because ions at lower *m/z* values can be detected in the *m/z* range of 400–2000, glycopeptide ions with higher *m/z* values might be missed to obtain product ion spectra. To detect glycopeptide ions preferentially, another LC-ESI-MS/MS analysis was carried out in the *m/z* range of 1000–2000 using an aliquot of 0.4 μg of the tryptic digest. Fig. 2A shows a total ion chromatogram (TIC) of a TOF-MS scan for the full scan *m/z* 1000–2000. Fig. 2B shows a TIC of the product ion scan. Because product ion spectra of glycopeptide precursor ions have abundant carbohydrate B-ions, *m/z* 204 (HexNAc), *m/z* 186 (HexNAc-H_2O), *m/z* 366 (HexHexNAc), and *m/z* 292 (NeuAc), the extracted ion chromatogram at *m/z* 204.05–204.15 (HexNAc, 204.08) of the product ion scan is illustrated in Fig. 2C. The extracted ion chromatogram at *m/z* 204.05–204.15 of product ion spectra provides a useful indication of the selection of glycopeptide precursor ions. The glycopeptide ions were assigned based on an examination of product ion spectra using the information on amino acid sequences of the peptides containing a putative N-glycosylation site.

Identification of Asn119 glycopeptide

The product ion spectrum of 1366.6 (+3) at 26 min, labeled by A in Fig. 2C, is shown in Fig. 3A. There were abundant oligosaccharide oxonium ions such as *m/z* 204 (HexNAc), *m/z* 366 (HexHexNAc), *m/z* 186 (HexNAc-H_2O), *m/z* 168 (HexNAc-2H_2O), *m/z* 274 (NeuAc-H_2O), and *m/z* 292 (NeuAc). Thus, this precursor ion was assigned as a glycopeptide. Several fragment ions consistent with b- and y-series fragment ions [24] derived from the peptide EHEGAIYPDN^{119}TTDFQR (residues 110–125) were detected together with several deamidated (−17) or dehydrogenated (−18) b- and y-series ions and y-series ions with the GlcNAc residue. Thus, the peptide moiety EHEGAIYPDNTTDFQR was suggested. The carbohydrate's molecular weight, 2223.0, was calculated by subtracting the theoretical molecular weight of the peptide (1891.8) from

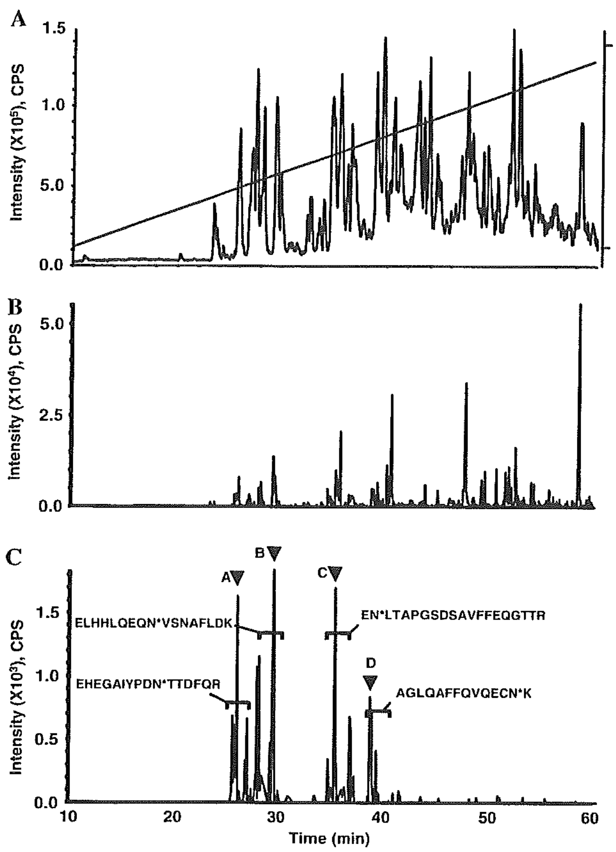

Fig. 2. LC-ESI-MS/MS in the *m/z* range of 1000–2000 of the tryptic digest of human CP. (A) TIC of the TOF-MS scan for the full-scan *m/z* 1000–2000 and the HPLC gradient. (B) TIC of the product ion scan acquired data-dependently. (C) Extracted ion chromatograph at *m/z* 204.05–204.15 of the product ion spectra. Brackets denote glycopeptide fraction and peptide sequences of the glycopeptides. Product ion spectra indicated by A–D are shown in Fig. 3.

the calculated molecular weight of the glycopeptide (4096.7) and adding the molecular weight of H_2O (18.0). The presence of product ions at *m/z* 274 (NeuAc-H_2O) and *m/z* 292 (NeuAc) suggested sialylation of the oligosaccharide. Thus, the carbohydrate's composition, $[HexNAc]_4[Hex]_5[NeuAc]_2$, was deduced.

Identification of Asn743 glycopeptide

The product ion spectrum of 1628.4 (+3) at 29 min, labeled by B in Fig. 2C, is shown in Fig. 3B. This precursor ion was assigned as a glycopeptide due to the presence of abundant oligosaccharide oxonium ions such as *m/z* 204 (HexNAc), *m/z* 366 (HexHexNAc), and *m/z* 292 (NeuAc) in the product ion spectrum. Several fragment ions were consistent with theoretical b- and y-series fragment ions derived from the peptide ELHHLQEQN^{743}VSNAFLDK (residues 735–751). Doubly charged ions of peptide (*m/z* 1011.7), peptide + HexNAc (*m/z* 1113.1), peptide + 2HexNAc (*m/z* 1214.6), peptide + 2HexNAc + Hex (*m/z* 1295.5), peptide + 2HexNAc + 2Hex (*m/z* 1376.7), and peptide + 2HexNAc + 3Hex (*m/z* 1457.5) showed the sequential fragmentation of the pentasaccharide carbohydrate core. The carbohydrate's molecular weight, 2879.1, was calculated from the theoretical molecular weight of the peptide (2021.0) and the calculated molecular weight of the glycopeptide (4882.1). The carbohydrate's composition, $[HexNAc]_5[Hex]_6[NeuAc]_3$, was deduced from the molecular weight.

Identification of Asn378 glycopeptide

The product ion spectrum of 1444.6 (+3) at 35 min, labeled by C in Fig. 2C, is shown in Fig. 3C. Abundant oligosaccharide oxonium ions were detected, as were several fragment ions consistent with b- and y-series fragment ions derived from the peptide EN^{378}LTAPGSDSAVFFEQGT TR (residues 377–391). The carbohydrate's molecular weight, 2222.9, was calculated from the theoretical molecular weight of the peptide (2126.0) and the calculated molecular weight of the glycopeptide (4330.9). Thus, the peptide moiety ENLTAPGSDSAVFFEQGTTR and the carbohydrate's composition, $[HexNAc]_4[Hex]_5[NeuAc]_2$, were suggested.

Identification of Asn339 glycopeptide

The product ion spectrum of 1282.6 (+3) at 39 min, labeled by D in Fig. 2C, is shown in Fig. 3C. The spectrum contains abundant oligosaccharide oxonium ions, and several fragment ions consistent with b- and y-series fragment ions derived from the peptide AGLQAFFQVQECN^{339}K (residues 327–340) were detected. The product ion spectrum contains the ions of the peptide (*m/z* 1640.8) and peptide + HexNAc (*m/z* 1843.9) and several y-series fragment ions of the peptide with a GlcNAc residue. The carbohydrate's molecular weight, 2223.0, was calculated from the theoretical molecular weight of the peptide (1639.7) and the calculated molecular weight of the glycopeptide (3844.7). Thus, the peptide moiety AGLQAFFQVQECNK and the carbohydrate's composition, $[HexNAc]_4[Hex]_5[NeuAc]_2$, were suggested.

Heterogeneity of oligosaccharides at each glycosylation site

Glycopeptides with the potential N-glycosylation sites Asn119, Asn339, Asn378, and Asn743 were detected, whereas no glycopeptides containing the other sites (Asn208, Asn569, and Asn907) could be detected in this LC-ESI-MS/MS analysis. These findings suggest that Asn119, Asn339, Asn378, and Asn743 of human CP are glycosylated and that Asn208, Asn569, and Asn907 are not. Once a glycopeptide was identified, the other glycopeptides with the same peptide could be easily assigned because they were eluted at a similar retention time in the order of the number of NeuAc and had similar product ion spectra and molecular weight difference of sugar units. The oligosaccharide heterogeneity at each four N-glycosylation sites was determined by mass spectrum. For a representative example, the mass spectrum of the glycopeptides containing

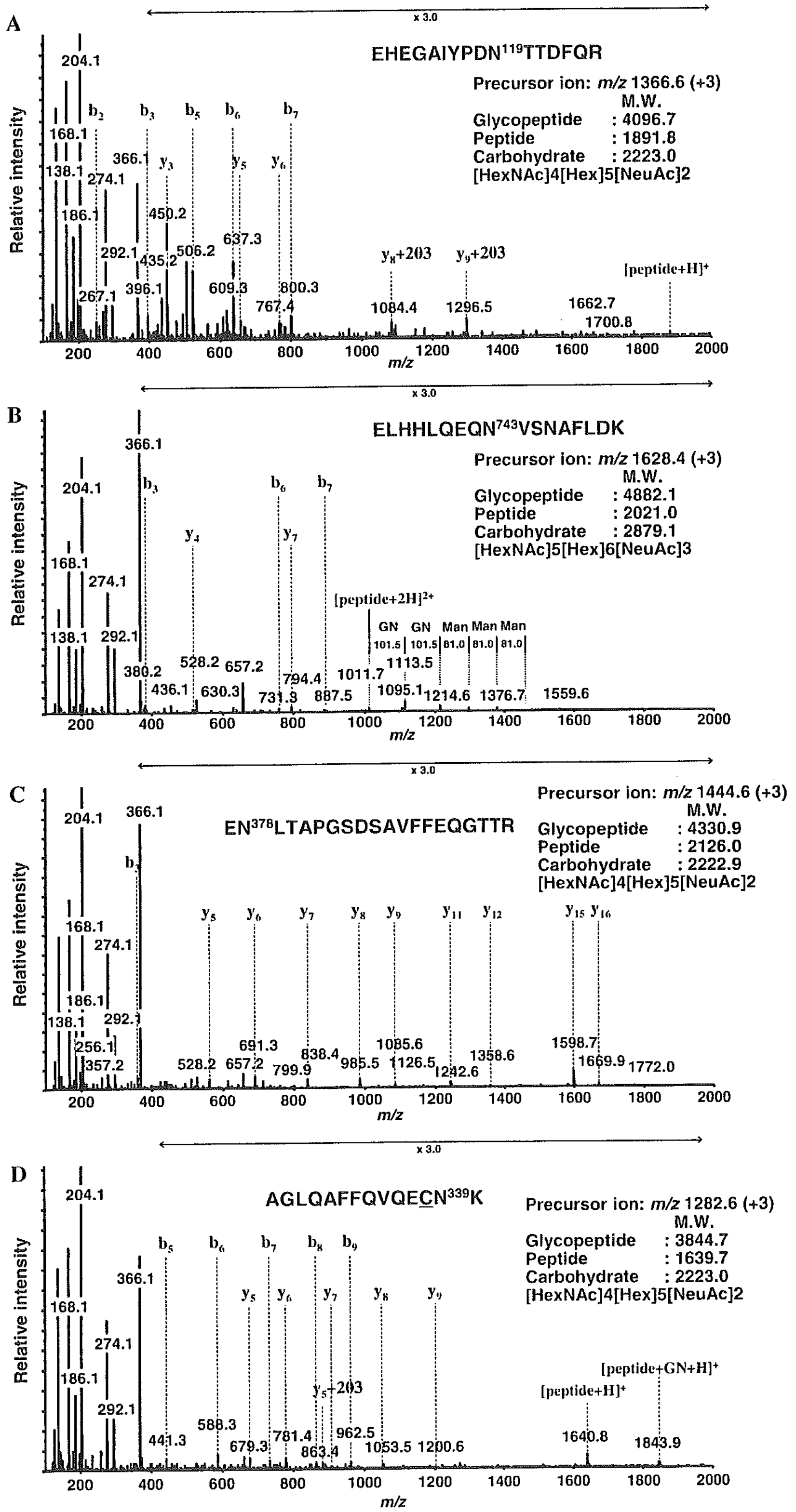

Fig. 3. Product ion spectra of *m/z* 1366.6 (+3) at 26 min (A), *m/z* 1628.4 (+3) at 29 min (B), *m/z* 1444.6 (+3) at 35 min (C), and *m/z* 1282.6 (+3) at 39 min (D) labeled by A, B, C, and D, respectively, in Fig. 2C. These spectra show abundant carbohydrate-derived ions at *m/z* 168 (HexNAc-2H_2O), *m/z* 186 (HexNAc-H_2O), *m/z* 204 (HexNAc), *m/z* 366 (HexHexNAc), *m/z* 274 (NeuAc-H_2O), and *m/z* 292 (NeuAc). The b- and y-series fragment ions [24] derived from the peptide moiety were observed. The molecular weights of the oligosaccharide were calculated from the molecular weights of the glycopeptide and peptide, and the deduced oligosaccharide composition is presented. Cystein residue was carboxymethylated.

Asn743 at 27.5 to 31.5 min is shown Fig. 4. The results of glycosylation analysis are summarized in Table 1. Deduced compositions of the oligosaccharides are estimated based on the calculated molecular weights of the oligosaccharides. Relative peak intensity was calculated by comparing triply charged glycopeptide ions. All glycosylation sites were occupied by at least three kinds of oligosaccharides, namely disialobiantennary structures ($[HexNAc]_4[Hex]_5[NeuAc]_2$), disialobiantennary structures with fucose ($[HexNAc]_4[Hex]_5[NeuAc]_2[Fuc]_1$), and trisialotriantennary structures ($[HexNAc]_5[Hex]_6[NeuAc]_3$). Trisialotriantennary structures with one fucose or two fucoses ($[HexNAc]_5[Hex]_6[NeuAc]_3[Fuc]_{1-2}$) were also detected at Asn119 and Asn743; furthermore, tetrasialotetraantennary structures with no fucose or one fucose ($[HexNAc]_6[Hex]_7[NeuAc]_4[Fuc]_{0-1}$) were detected at Asn743.

Linkage analysis of oligosaccharides by exoglycosydase digestion

To elucidate the oligosaccharide structure in terms of sequence and linkage, aliquots of the tryptic digest were further digested with exoglycosidases. As a representative example, Fig. 5 shows integrated mass spectra during the periods at which Asn119 glycopeptides were eluted in LC-ESI-MS analyses before and after digestion with exoglycosidase arrays. Treatment with α2–3 neuraminidase removed one NeuAc residue from most of the triantennary structures ($[HexNAc]_5[Hex]_6[NeuAc]_3[Fuc]_{0-2}$) and a small amount of biantennary structures ($[HexNAc]_4[Hex]_5[NeuAc]_2[Fuc]_{0-1}$) (Fig. 5B). A minor amount of triantennary structures removed two NeuAc residues. Thus, it appears that most triantennary structures contain one α2–3-linked NeuAc. Treatment with α2–3 neuraminidase + β1–4 galactosidase removed all terminal galactose residues from the desialylated glycans without fucose residues but only partially digested terminal galactoses from the desialylated glycans with fucoses (Fig. 5C). The addition of α1–3,4 fucosidase to α2–3 neuraminidase + β1–4 galactosidase treatment completely digested the remaining terminal galactose by releasing one fucose and one galactose (Fig. 5D). Thus, galactose residues are linked β1–4 to GlcNAc, and undigestion of terminal galactose by β1–4 galactosidase is due to attachment of fucose [25,26]. Because galactose was linked to GlcNAc in the β1–4 position, the fucose removed with α1–3,4 fucosidase may be linked α1–3 to GlcNAc but not α1–4 to GlcNAc. These data strongly suggested that sialyl Lewis X structure was present in human CP. Sialyl Lewis X structure was present predominantly in triantennary oligosaccharides, but a small amount seemed to be present in biantennary oligosaccharides as well. The remaining fucose residue may be linked α1–6 to reducing end GlcNAc (core fucose).

Fig. 6 shows integrated mass spectra of Asn119, Asn743, Asn378, and Asn339 glycopeptides in LC-ESI-MS analysis following digestion with α2–3,6,8,9 neuraminidase + β1–4 galactosidase. Treatment with α2–3,6,8,9 neuraminidase + β1–4 galactosidase removed all NeuAc and then removed terminal galactoses in the outer arms without fucose. Thus, this treatment could differentiate glycoforms based on the location of fucose residues. Fucosylation occurred predominantly at reducing end GlcNAc in biantennary oligosaccharides and occurred at reducing end GlcNAc and/or outer arm GlcNAc in triantennary oligosaccharides. Mass spectra of Asn119 and Asn743 glycopeptides showed higher oligosaccharide heterogeneity, and a minor amount of tetraantennary glycans could be detected. The glycosylation profile

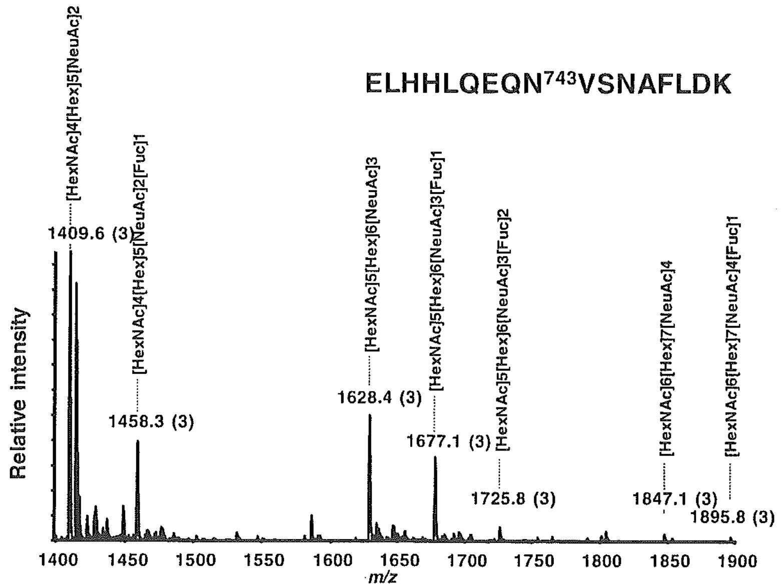

Fig. 4. Mass spectrum of the glycopeptides containing Asn743 eluting at 27.5–31.5 min from Fig. 2A. Deduced composition of the oligosaccharides is indicated based on the molecular weights of the oligosaccharides.